Anticipated Degradation Modes of Metallic Engineered Barriers for High-Level Nuclear Waste Repositories

Martín A. Rodríguez

JOM
The Journal of The Minerals, Metals & Materials Society (TMS)

ISSN 1047-4838
Volume 66
Number 3

JOM (2014) 66:503-525
DOI 10.1007/s11837-014-0873-7

Springer

JOM, Vol. 66, No. 3, 2014
DOI: 10.1007/s11837-014-0873-7

Anticipated Degradation Modes of Metallic Engineered Barriers for High-Level Nuclear Waste Repositories

MARTÍN A. RODRÍGUEZ[1,2,3]

1.—Consejo Nacional de Investigaciones Científicas y Técnicas, Gerencia Materiales, Comisión Nacional de Energía Atómica, Instituto Sabato, UNSAM/CNEA, Av. General Paz 1499, B1650KNA San Martín, Buenos Aires, Argentina. 2.—e-mail: martinrz@gmail.com. 3.—e-mail: maalrodr@cnea.gov.ar

Metallic engineered barriers must provide a period of absolute containment to high-level radioactive waste in geological repositories. Candidate materials include copper alloys, carbon steels, stainless steels, nickel alloys, and titanium alloys. The national programs of nuclear waste management have to identify and assess the anticipated degradation modes of the selected materials in the corresponding repository environment, which evolves in time. Commonly assessed degradation modes include general corrosion, localized corrosion, stress-corrosion cracking, hydrogen-assisted cracking, and microbiologically influenced corrosion. Laboratory testing and modeling in metallurgical and environmental conditions of similar and higher aggressiveness than those expected in service conditions are used to evaluate the corrosion resistance of the materials. This review focuses on the anticipated degradation modes of the selected or reference materials as corrosion-resistant barriers in nuclear repositories. These degradation modes depend not only on the selected alloy but also on the near-field environment. The evolution of the near-field environment varies for saturated and unsaturated repositories considering backfilled and unbackfilled conditions. In saturated repositories, localized corrosion and stress-corrosion cracking may occur in the initial aerobic stage, while general corrosion and hydrogen-assisted cracking are the main degradation modes in the anaerobic stage. Unsaturated repositories would provide an oxidizing environment during the entire repository lifetime. Microbiologically influenced corrosion may be avoided or minimized by selecting an appropriate backfill material. Radiation effects are negligible provided that a thick-walled container or an inner shielding container is used.

INTRODUCTION

High-Level Waste

Radioactive waste is classified according to the specific activity and the half-lives of the radionuclides contained in the waste. High-level waste (HLW) contains levels of activity concentration high enough to generate significant quantities of heat by radioactive decay and large amounts of long lived radionuclides. HLW typically has levels of activity concentration in the range of 10^4–10^6 TBq/m^3 (1 Bq: one disintegration per second) and contains radionuclides with half-lives of more than 30 years. HLW comes from the nuclear power production, either as spent fuel (if it is declared waste) or as conditioned waste arising from the reprocessing of spent fuel, research facilities, disused sealed sources, and defense programs. HLW requires a great degree of containment and isolation from the accessible environment to ensure long-term safety.[1]

Geological Repositories

The selected worldwide alternative for the final disposal of HLW is the deep geological isolation in underground repositories comprising a multibarrier system made of engineered and natural barriers. Geological repositories located in a stable host rock must provide public safety, protection of the environment, and security from accidental or deliberate intrusion. The multibarrier system

(Published online February 1, 2014)

should contain the radionuclides, allowing them to decay and eventually limit their release to the environment. This system is fully effective only after closure of the repository. Closure is attained when all barriers considered in the repository design are emplaced and all the underground openings are backfilled and sealed. Repository facilities may not operate under institutional control due to the long time scale of the required waste isolation. However, some waste management national programs (WMNPs) may require that the waste remains retrievable for some time until the decision of closure is taken. The retrievability period may extend even after backfilling and sealing of the repository, but indefinite institutional control is not viable.[2,3]

Suitable geological environments for disposal of long-lived radioactive waste vary considerably in their nature. The host rocks include diverse types loosely categorized as crystalline rocks (Canada, Finland, and Sweden), argillaceous rocks (France, Switzerland, and Belgium), salt rock (Germany), and volcanic rock (United States). The selected host rock will determine the groundwater environment. Groundwater will be the carrier of radionuclides away from the repository as solutes. Once a suitable geological environment for disposal has been selected, the engineered barrier system (EBS) is designed to take advantage of the main features of the environment. The EBS includes the waste form, the waste package and overpack, and the backfill/buffer materials. The waste form may be the conditioned spent fuel or waste conditioned in a glass, bitumen, or cement matrix. The waste package is the container where the waste form is placed for different purposes such as short-term containment during transport and/or storage to shielding and longer term containment. These packages can consist of untreated or treated and conditioned waste in steel drums, concrete containers, casks, or other metallic containers. The waste package is surrounded by an overpack, which is an outer corrosion-resistant barrier. This waste container or canister is the only absolute barrier of the multibarrier system. Most of the repository designs include a backfill/buffer material emplaced immediately around the waste containers that fills and seals the tunnels and shafts. The backfill/buffer material is generally cement, crushed salt, or a highly compacted bentonite that may be mixed with sand. Finally, the EBS is completed by the repository mass backfill in and around the region used for waste emplacement (generally a mixture of crushed rock and clay). The EBS is called the near field, which is the part of the system significantly affected by the presence and emplacement of the waste. The natural barriers are called the far field, while the biosphere is treated separately. The role of the natural and engineered barriers may vary significantly in different repository concepts. The ultimate goal is the overall safety of disposal and not the performance of single barriers. However, the concept of redundancy in isolation capacity among the various barriers is often invoked by the WMNP.[2–5]

Metallic Engineered Barriers

This article particularly focuses on those metallic barriers meant for corrosion resistance (not to give mechanical strength or radiation shielding, although some of them may also provide these features). The performance of the corrosion-resistant barriers is mainly affected by the near-field conditions. The main (but not necessarily the only) corrosion-resistant engineered barrier is the overpack, also called waste container or canister. The waste container is an absolute barrier because it is intended to contain the radionuclides in the waste completely for a certain period of time. The other barriers control the rate at which the radionuclides can be mobilized and released into the surrounding rock. For most categories of long-lived waste, a complete containment period of some hundreds of years is enough for a significant activity reduction. However, the length of required containment varies among WMNP between 500 years and 10^6 years.[2,4–9]

The most advanced projected repositories may be loosely categorized in two types according to the corrosive environment in contact with the waste containers:

- Saturated repositories: They are located below the water table (Sweden, Finland, Canada, Germany, France, Switzerland, Belgium, Spain, United Kingdom, and Japan). With the exception of the French repository model, the EBS may include a backfill of compacted bentonite (Sweden, Finland, Canada, Switzerland, Spain, and Japan), a cementitious material (Belgium), or a crushed salt (Germany). Following its closure, the groundwater regime may be progressively re-established and the whole system may saturate. Rock stresses may equilibrate and lithostatic loads may be transferred to some parts of the EBS. The operational pressure may be higher than the atmospheric pressure (>10 MPa). The remaining oxygen in trapped air may react with the rock and EBS materials. Reducing conditions may prevail after an initial period of oxygen consumption. With the exception of the likely German repository model, the temperature peak is limited to 100°C.[3]
- Unsaturated repositories: They are located above the water table (such as the initially designed Yucca Mountain, United States). The EBS does not include the backfill of tunnels. An additional corrosion-resistant barrier is considered (drip shield) to avoid or delay the contact of seepage water with the waste container. The operational pressure may be near the atmospheric pressure. Oxidizing conditions may prevail over the entire repository lifetime because oxygen may freely

reach the waste containers surface. The temperature peak may exceed the boiling point of water. Deliquescent salts may allow corrosion of containers at temperatures above 100°C.[5]

The characteristics of the environment in contact with the waste containers and its evolution in time are relevant to anticipate the corrosion modes of the selected material throughout the repository lifetime. Regarding the selection of a container material for a given environment, the two conceptual approaches are as follows:[10–12]

- Corrosion allowance: Selection of readily corrodible metals (e.g. carbon steel and lead) with sufficient thickness to delay container failure until the short-lived fission products in the waste have decayed (~1000 years).
- Corrosion resistance: Selection of corrosion-resistant materials (e.g., copper, stainless steels, nickel alloys, and titanium alloys) that are intended to prevent water access until all the most mobile radionuclides have decayed (~10^4–10^6 years). Stainless steels, nickel alloys, and titanium alloys form stable passive films kinetically resistant to corrosion, while copper in a reducing environment is thermodynamically immune to corrosion. They usually need internal structural support.

The approach explained above depends not only on the selected material but also on the environment. Carbon steel embedded in a cement matrix may be considered as corrosion resistant, while copper in an oxidizing environment would be a case of corrosion allowance. Figure 1 shows the galvanic series of various materials in seawater. Although this environment may be quite different from the service environments in repositories, a comparison of the open circuit or corrosion potentials (E_{CORR}) of materials is still useful. Candidate materials for waste containers are marked by arrows in Fig. 1. The selected materials cover a wide range of E_{CORR}. Passive alloys such as titanium, Ni-Cr-Mo, Ni-Fe-Cr, and stainless steels have noble E_{CORR} values, while low and mild alloy steels and cast iron have active E_{CORR} values. E_{CORR} values for copper, aluminum bronze, 70–30 Cu-Ni, 90–10 Cu-Ni, and lead lie in an intermediate range of potentials. 70–30 and 90–10 Cu-Ni are considered as alternative materials by the German repository model.[6] Copper, 70–30 Cu-Ni, and aluminum bronze were considered by the U.S. repository model.[13] Lead was considered as a corrosion allowance material by a former Argentinean repository model.[14] However, it was discarded because of its poor mechanical properties and the repository project was terminated.[3]

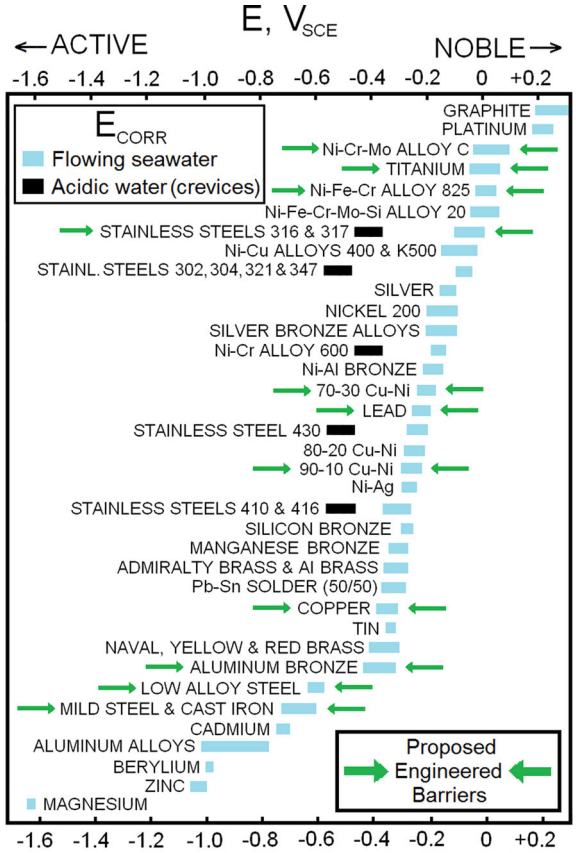

Fig. 1. Galvanic series of various materials in flowing seawater (2.5–4 m/s) at temperatures in the range from 5°C to 30°C (adapted from Ref. 15).

Metallurgical and Environmental Conditions

The many factors affecting the corrosion performance of candidate materials in the corresponding repository environment may be classified in the two following groups:

- Metallurgical (internal) conditions: They depend on the material chemical composition, microstructure, processing and finishing and all the processes involved on the construction, storage and transportation of the waste container. These factors include the mill annealing process (bright or black annealing), the presence of a weld seam containing a cast or dendritic microstructure and a heat-affected zone (HAZ), postwelding treatments, metal finishing (roughness and defects), thermal aging treatments, presence of high temperature or air-formed oxides, residual stresses, and so on.
- Environmental (external) conditions: They depend on the characteristics of the repository environment including the groundwater system, the natural barriers, and the EBS. The near-field conditions are the most relevant and they are determined by the interaction of the backfill (if there is any) with the surrounding rock and groundwater system. Groundwater flow processes control the rate at which water can enter the near field and the water chemistry. However, the chemistry of water in contact with the containers

is more affected by the selected backfill material. The environmental factors include chemical composition of the solution in contact with the containers (aggressive and inhibitor species, oxygen and pH), temperature, pressure, microbial activity, volume of electrolyte in contact with the containers, debris or deposits forming crevices, radiation field, radiolysis products, applied stresses, and so on.

The life prediction of the waste containers needs the assessment of the degradation modes suffered by the container in the corresponding metallurgical conditions and the evolution of the environmental conditions over time. This article reviews the anticipated degradation modes of the metallic barriers considered for HLW repositories in the environments selected by the most advanced WMNP.[2] For those readers interested in life prediction of waste containers, there is another article dealing with this topic in this issue of *JOM*. This review is organized by the considered material types: copper alloys, carbon steel, stainless steels, nickel alloys, and titanium alloys. The degradation modes commonly considered by the WMNP include general corrosion, localized corrosion (pitting and crevice corrosion), stress-corrosion cracking (SCC), hydrogen-assisted cracking (HAC), and microbiologically influenced corrosion (MIC). Corrosion during storage in a stage previous to the final disposal of containers is not considered in this review. Some degradation modes may be ruled out by the material/environment selection. The degradation modes refer to particular phenomenologies but not necessarily to precise or known degradation mechanisms.

COPPER ALLOYS

Copper was the first material proposed as a corrosion-resistant container for the disposal of HLW.[16] The current alloy specification is oxygen-free Cu (UNS C10100) with the addition of up to 100 ppm of phosphorus to improve the resistance to creep.[17] This alloy is commonly called OFP Cu. Copper has generally been proposed as a waste container in conjunction with highly compacted bentonite backfill in saturated repositories.[6] Currently, OFP Cu is the selected or reference container material of WMNP in Sweden, Finland, and Canada, and it is the alternative material of WMNP in Germany, Japan, the United Kingdom, Spain, and Switzerland. The Swedish and Finnish models are among the most advanced worldwide repository projects. Although other copper alloys have been proposed for waste containers, there is little research in relevant conditions and they are not included in the current review.[6]

General Corrosion

The mechanism of the general corrosion of copper in chloride-containing compacted bentonite has been studied in some detail.[7,18–20] Figure 2 shows the reaction schemes for the corrosion of copper in compacted bentonite saturated with oxygen considering the reactions involving sulfide. In O_2-containing chloride environments, Cu dissolves reversibly via an adsorbed intermediate ($CuCl_{ADS}$) to produce a dissolved cuprous complex ($CuCl_2^-$). Disregarding the effect of sulfide, the cathodic reaction sustaining corrosion is oxygen reduction. It occurs irreversibly on the Cu surface by a four-electron process producing OH^-. The detailed mechanism depends on the interfacial pH and the presence of catalytic surface intermediates, among other factors. Both anodic and cathodic reactions are under transport control in compacted bentonite. Consequently, E_{CORR} is insensitive to the detailed interfacial oxygen-reduction mechanism. Cu^{2+} may act as an oxidant via an irreversible interfacial reduction process. The cupric species are formed from the oxidation of $CuCl_2^-$ by O_2. Anodic dissolution of Cu only leads to cuprous species that are stabilized as chloride complexes. Fe^{2+} is expected in the pore water due to the dissolution of minerals in the rock and clay, such as biotite, magnetite, and pyrite. Fe^{2+} may react with Cu^{2+} or with dissolved O_2 leading to Fe^{3+}. The latter reaction is responsible for the expected evolution to anaerobic conditions in the repository.[17,19,20]

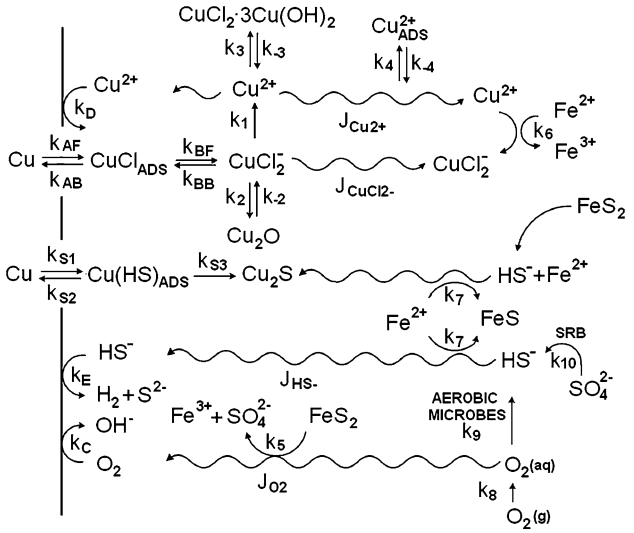

Fig. 2. Reaction schemes for the corrosion of copper in contact with compacted bentonite in oxygenated saline groundwater considering the reactions involving sulfide (adapted from Ref. 20).

Precipitation of corrosion products is expected at the Cu/bentonite interface due to their slow diffusion in the compacted bentonite. The corrosion products form a duplex film comprising an inner layer of Cu_2O and an outer green layer of atacamite ($CuCl_2{\cdot}3Cu(OH)_2$). Depending on the relative concentration of CO_3^{2-} and Cl^- in the pore water, malachite ($Cu_2CO_3(OH)_2$) may form instead of atacamite. Although atacamite and malachite are

electrically insulating, this outer layer is porous and noncontinuous. O_2 reduction may proceed on the inner Cu_2O layer. These corrosion products are not protective, allowing the corrosion of the underlying copper surface.[21]

Na-bentonite is cation exchanging and possesses a net negative surface charge. Cupric species (Cu^{2+}, $CuOH^+$, or $CuCl^+$) are strongly adsorbed, but the negatively charged cuprous $CuCl_2^-$ is not adsorbed at all. These adsorption and desorption processes are accounted in models because they have significant impact on the corrosion of Cu in compacted buffer material. The possibility of O_2 consumption by aerobic microbes is also included in modeling. The mass transport of solutes in the near field occurs only by diffusion. Convective mass transport is not expected.[18–20]

In the absence of sulfide, corrosion of Cu would stop after the consumption of the O_2 initially trapped in the repository (and any Cu^{2+}).[7,18,19] In the Swedish/Finnish model, this period may last 200 years, whereas the projected container lifetime is $\sim 10^5$ years.[19] However, if HS^- is present, highly insoluble Cu_2S may form, which reduces the Cu^+ activity and hence the Cu/Cu^+ equilibrium potential. Consequently, H_2O (or HS^-) becomes an oxidant for Cu with the accompanying evolution of H_2. The reaction scheme involving sulfide is shown in Fig. 2. In the presence of HS^-, Cu dissolves via a two-step process. The first step is fast and involves the reversible formation of an adsorbed intermediate ($Cu(HS)_{ADS}$). The second step is rate controlling and leads to the irreversible formation of Cu_2S. Cu_2S (chalcocite) forms a layer on the copper surface. In solutions with a high chloride to sulfide concentration ratio, this film possesses a cellular structure. The cathodic reactions sustaining corrosion are the reductions of HS^- and/or H_2O to H_2.[22–25] The sources of sulfide include groundwater, sulfide-containing minerals (pyrite), and reduction of sulfate by sulfate-reducing bacteria (SRB). Microbial activity is not expected at the container surface because it is suppressed in highly compacted bentonite. However, SRB may act within the far field and HS^- may diffuse to the container surface from the groundwater. The estimated rate for this transport-limited corrosion process is slower than 1 nm/year.[7,19,20]

Copper might suffer corrosion in O_2-free solutions with high Cl^- content, low pH (pH < 5–6), and high temperature (80–100°C). This possibility has been stated on thermodynamic grounds and it is indicated in Eq. 1. The calculations in environmental conditions relevant for the repository indicate a concentration of dissolved Cu lower than 10^{-6} mol/kg at the equilibrium for a closed system. In a semiclosed system such as the repository, the corrosion rate would be given by the diffusion rate of the corrosion products away from the container surface through the bentonite.[17]

$$Cu + H^+ + nCl^- \longleftrightarrow {}^1/_2H_2 + CuCl_n^{(1-n)} \qquad (1)$$

The thermodynamic stability of copper in the absence of O_2 and HS^- has been questioned, indicating that Cu may suffer corrosion in pure water with the sustained evolution of hydrogen.[26–28] The classic thermodynamic approach indicates that Cu will corrode in pure water only until the equilibrium partial pressure of H_2 in Eq. 2 is attained. The equilibrium partial pressure of H_2 is of the order 10^{-11} Pa at 25°C. Because the partial pressure of H_2 in the atmosphere is much higher than this value, corrosion may not occur under ambient conditions.

$$2Cu + H_2O \longleftrightarrow Cu_2O + H_2 \qquad (2)$$

However, Hultquist et al.[28,29] indicated that Eq. 2 is not correct because a different solid phase forms (H_xCuO_y, equivalent to CuOH for $x = y = 1$). According to these authors, H_xCuO_y is thermodynamically stable, as the equilibrium partial pressure of H_2 is of the order of 100 Pa at 60–70°C. They report anaerobic corrosion rates for Cu of ~ 5 μm/year. The original observations of Hultquist et al. have been very difficult to reproduce. A considerable amount of work has been devoted to this topic without reaching a definite agreement.[26–28,30,31] Even considering the mechanism proposed by Hultquist et al. the consequences for the corrosion of copper in the repository are minor. Dissolved H_2 possesses a low diffusivity through compacted bentonite forming a gas phase. The equilibrium partial pressure of H_2 would be quickly attained and the corrosion rate of Cu then would be controlled by the slow diffusion of dissolved H_2 through the bentonite. As in the case of sulfide corrosion, the estimated corrosion rate for this process is lower than 1 nm/year.[19,31]

Localized Corrosion

Pitting corrosion may occur only if E_{CORR} of the metal or alloy is higher than its corresponding pitting potential (E_P) in a given environment. The difference (E_P–E_{CORR}) is frequently used as a safety margin for localized corrosion. In a more conservative approach, the pitting corrosion repassivation potential (E_{RP}) might be used instead of E_P. This latter approach has not been used for copper, and relatively few values of E_{RP} are available in relevant conditions. It is reported that E_P decreases as the temperature increases. However, E_{CORR} also decreases with temperature, leading to a larger (E_P–E_{CORR}) difference at higher temperatures. In fact, the Cu tendency to localized corrosion decreases with temperature.[13,17,32]

Three types of pitting have been recognized for copper in water distribution pipes. Type I pitting is associated with cold, hard, and moderately hard water containing HCO_3^-, SO_4^{2-}, Cl^-, and O_2. A carbon film formed during the bright annealing of

the copper tube is thought to be necessary for Type I pitting. Pit initiation involves the formation of a CuCl pocket underneath a porous Cu_2O film. The dissolved Cu^+ is oxidized to Cu^{2+} by O_2 and precipitates forming a crust of $CuCO_3{\cdot}Cu(OH)_2$ and $CaCO_3$.[17] The crust forms an occluded region in which localized dissolution continues. E_P lies between 0.060 V_{SCE} and 0.170 V_{SCE}. Type I pitting produces hemispherical pits. Type II pitting is associated with hot potable water with pH < 7.4 and a concentration ratio of $[HCO_3^-]/[SO_4^{2-}] < 1$. It produces pits with a larger depth/width ratio than type I pitting. E_P lies between 0.115 V_{SCE} and 0.160 V_{SCE}. Type III pitting is induced by microbial activity, and it is not considered here. In all cases, O_2 is needed for pit propagation to occur. Consequently, pitting corrosion of Cu is not expected in the anaerobic stage of the repository. The role of O_2 is as follows: (I) It is the oxidant supporting pit growth; (II) it oxidizes Cu^+ to Cu^{2+}, providing another oxidant; and (III) it reduces to OH^- producing a local alkalinity, which helps to maintain the crust over the pit avoiding the dilution of the local pit chemistry. It is not clear whether O_2 reduction occurs on a large cathodic area or only above the pit. Pitting of copper pipes in water distribution systems is sustained by the high O_2 concentration and its continual replenishment. The likelihood of pitting corrosion in the repository environment decreases as the trapped O_2 is consumed.[17,32]

Stable propagation of pitting corrosion of Cu has been modeled based on mass transport and chemical equilibrium principles. Pitting corrosion propagation depends on the transport of both reactants to the bottom of the pit and dissolved Cu out of the pit. The transport of dissolved Cu out of the pit must be fast enough to avoid the formation of protective corrosion products that lead to the pit death. Calculations indicate that the fraction of transported Cu out of the pit must be higher than 40% if Cu_2O precipitates within the pit and higher than 70% if CuCl precipitates. The potential at which the transported fraction of dissolved Cu equals the critical value is the minimum potential for pit propagation. Figure 3 shows the predicted conditions of potential and chloride concentration for pit propagation to occur.[17]

OFP Cu is reported to be free from localized corrosion after 18 months of exposure to saturated bentonite at 50°C, 75°C, and 100°C. However, Cu-30Ni suffered localized attack at 75°C and 100°C, showing penetration depths up to 25 μm.[6]

The near-field environment in the repository is not expected to lead to classic pitting corrosion of the copper containers. Instead, some roughening of the surface has been observed after 2 years of exposure in aerated synthetic groundwater. The observed surface profile is explained by a mechanism involving initiation, growth, and death of pits. Pit death results from the decrease of the cathode to anode ratio due to (I) cathode blocking by the precipitation of insulating carbonates because of a local pH increase (II) dilution of the pit critical chemistry due to opening of the pit cover, or (III) the coalescence of adjacent pits resulting in a lateral growth. In the repository conditions, the spatial separation between anodic and cathodic processes is not permanent. However, the container surface might be nonuniformly wetted during the saturation stage. Consequently, application of these results is not straightforward.[19]

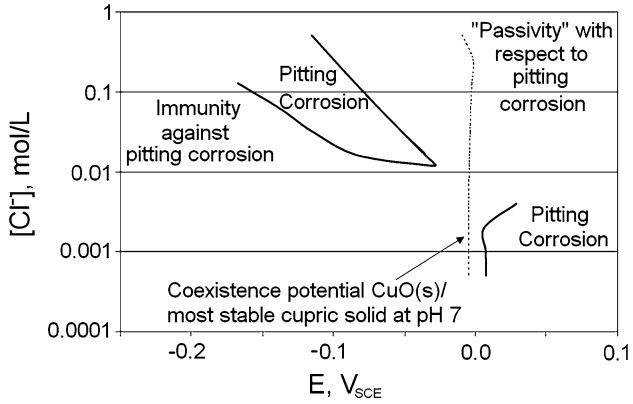

Fig. 3. Potential versus chloride concentration diagram identifying conditions for pitting corrosion propagation (adapted from Ref. 17).

Crevice corrosion by local acidification is unlikely to occur because the hydrolysis of Cu^+, especially when complexed by Cl^-, is weak. Cu^{2+} hydrolyzes more strongly than Cu^+. However, Cu^{2+} formation requires the presence of O_2, which is totally exhausted in crevices. Crevice corrosion of pure Cu may occur via a differential Cu^+ concentration cell mechanism. This form of localized corrosion is inherently self-limiting.[17]

Stress-Corrosion Cracking

SCC needs residual or applied tensile stresses on the material to occur. The distribution of tensile stress on the container as well as the effect of weld seams and postweld treatments (if there is any) are worth studying for all the considered materials. SCC of OFP Cu may occur in a few environments, including ammonium, nitrite, and acetate solutions. None of these species is naturally present in the repository environment, but they may be produced by microbial activity or introduced during repository construction. The presence of any of these species in the near field in concentrations high enough to produce SCC is unlikely. High chloride concentration and high temperature decreases the SCC susceptibility of Cu. E_{CORR} and interfacial pH must lie above the Cu_2O/CuO equilibrium line for SCC to occur. Consequently, SCC caused by ammonium, nitrite, and acetate is only viable within the initial aerobic stage. During the long-term anaerobic stage, sulfide has been identified as a possible aggressive agent causing SCC on Cu.

Copper is reported to be susceptible to SCC in sulfide solutions at $[HS^-] > 0.005$ mol/L.[33] As stated, when describing general corrosion, the flux of HS^- from the environment and its concentration at the container surface may be extremely low to support SCC. Recent research provides evidence of internal diffusion of sulfides into grain boundaries of OFP Cu, which should be assessed in the future.[34] Unlike OFP Cu, Cu-30Ni may be susceptible to SCC in granitic bentonite water.[6]

A comprehensive review of various postulated SCC mechanisms led to the conclusion that none of them would lead to SCC during the long-term anaerobic stage. The failure of a copper container in compacted bentonite by SCC is considered highly unlikely.[17,19,35,36]

Microbiologically Influenced Corrosion

There is strong evidence that microbial activity is suppressed in highly compacted bentonite. Biofilm formation is not expected within the near field. There is no agreement on the precise mechanism by which compacted bentonite avoids microbial activity. It may be either the mechanical effect of the swelling pressure or the low water activity in the pores. Although classic MIC is not expected, SRB may produce HS^- in the far field and it may diffuse to the container surface as explained above.[37]

Radiation Effects

The near-field environment may be influenced by the gamma radiation field outside the waste container. Radiation may cause radiolysis of gases and aqueous solutions in contact with the container. The radiation is dominated by the decay of ^{137}Cs, which has a half-life of 30 years. However, the design considered by the Swedish and Finnish models results in a dose rate of 0.5 Gy/h (1 Gy: 1 J of absorbed energy by kg of matter) at the container surface immediately after encapsulation and a negligible dose rate after a few hundred years. In these conditions, the influence of radiation may be negligible.[17]

CARBON STEEL

Presently, carbon steel (C-steel) is the selected or reference container material of WMNP in Belgium, France, Switzerland, Japan, Germany, and Spain, and it is the alternative material of WMNP in the United Kingdom and the United States. In most cases, specific grades of C-steel have not been defined because most WMNP are at an early stage of development. The German and Spanish WMNP have defined DIN TStE 355 C-steel as a reference material.[6]

C-steel is more suitable for use in repositories located in the saturated zone with limited O_2 availability. However, A588 low-alloy C-steel was initially considered an alternative waste container material for the Yucca Mountain repository.[38] Thick walls of C-steel may also provide structural support and radiation shielding besides corrosion allowance. C-steel has been proposed along with different types of backfill materials such as compacted bentonite (Switzerland, Japan, and Spain), cement (Belgium), crushed salt (Germany), or no backfill (the United States and France).

Corrosion of C-Steel in Bentonite and Argillaceous Environments

General Corrosion

The Japanese repository model may use a mixture of 70% bentonite/30% silica sand as a buffer material.[39] The Swiss model indicates a granular bentonite backfill in the sedimentary Opalinus clay.[40] The containers of the French repository may be in contact with groundwater from the Callo-Oxfordian clay.[12] In these environments, C-steel may suffer aerobic conditions until the trapped O_2 is consumed. After this initial aerobic stage, it may corrode anaerobically with the evolution of H_2. Active corrosion is expected for C-steel in bentonite because the pH of pore water (pH 7–8) is not high enough to passivate the metal.[39,41,42] The aerobic corrosion rate of C-steel is maximum at $[Cl^-] = 0.5$ mol/L and at 80°C.[41] Corrosion penetration caused by aerobic corrosion may be conservatively calculated by assuming that all the O_2 reacts with the C-steel container. This assumption leads to an average penetration depth of 0.3–1.8 mm for the Japanese model.[39]

Figure 4 shows the corrosion products formed on C-steel in aerobic, anaerobic, and carbonate-containing environments and their evolution. Aerobic corrosion of C-steel results in Fe^{3+} corrosion products such as goethite (α-FeOOH) and lepidocrocite (γ-FeOOH). Their crystallization may lead to the formation of maghemite (γ-Fe_2O_3) or hematite (α-Fe_2O_3). Fe^{3+} species also result from homogeneous oxidation of Fe^{2+} by O_2. As the initially trapped O_2 is consumed, Fe^{3+} species may be transformed to magnetite (Fe_3O_4) via reaction with dissolved Fe^{2+} Eq. 3 or via Fe^{3+} reduction coupled to Fe dissolution Eq. 4. Anaerobic corrosion of C-steel produces $Fe(OH)_2$, which may transform to Fe_3O_4 via the Schikkor reaction Eq. 5. In carbonate/bicarbonate solutions, $FeCO_3$ may form. Other types of rust are formed in sulfate and chloride solutions.[9,41,43]

$$2FeOOH + Fe^{2+} \rightarrow Fe_3O_4 + 2H^+ \quad (3)$$

$$2FeOOH + Fe + 2H_2O \rightarrow 3Fe(OH)_2 \rightarrow Fe_3O_4 + 2H_2O + H_2 \quad (4)$$

$$3Fe(OH)_2 \rightarrow Fe_3O_4 + 2H_2O + H_2 \quad (5)$$

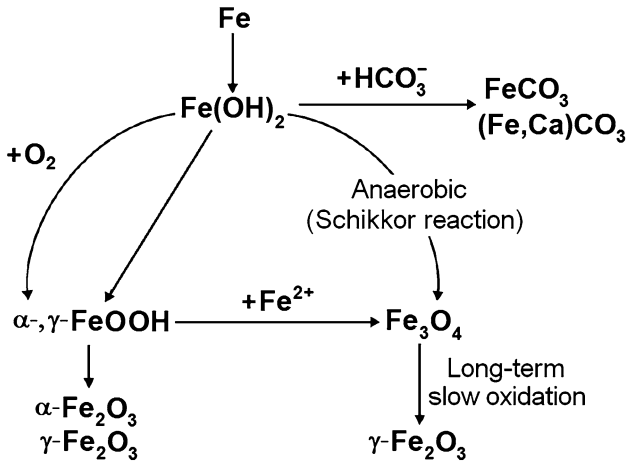

Fig. 4. Summary of formation and transformation of corrosion products on carbon steel in different environments (adapted from Ref. 9).

Some works provide evidence of magnetite producing an increased corrosion rate of C-steel, while other works indicate the opposite.[39,41,44] Nakayama et al.[45] indicate a corrosion rate of 0.9 mm/year for C-steel due to Fe_3O_4 reduction. Anaerobic corrosion rates of C-steel are higher in compacted bentonite than in bulk solutions. The absorption of Fe^{2+} by the clay may affect the protectiveness of the surface film. The film composition and structure are also different, with carbonate species incorporated into a dense product layer in bentonite compared with the compact Fe_3O_4 film formed in bulk solutions.[46] Anaerobic corrosion rates of C-steel decrease to values of 1–5 μm/year after several years of exposure. These values are not very sensitive to water chemistry.[12,39,41,46] The French national program provides an assessment of the corrosion rate (CR) of C-steel as a function of temperature (T). Equations 6 and 7 indicate the CR (in mm/year) as a function of T (in K) for the aerobic and anaerobic conditions, respectively; R is the gas constant.[12] However, other authors indicate that the corrosion rates of C-steel in anaerobic neutral conditions are insensitive to temperature.[41]

$$\mathrm{CR\,[mm/year]} = 1.042\exp(-11.1\ \mathrm{kJ/mol}/RT) \quad (6)$$

$$\mathrm{CR\,[mm/year]} = 0.162\exp(-10.8\ \mathrm{kJ/mol}/\mathrm{R}T) \quad (7)$$

Anaerobic corrosion of C-steel may produce Fe^{2+}, which may interact unfavorably with bentonite. The swelling ability of montmorillonite (a component of the bentonite) may be damaged, leading to nonswelling clay. This negative impact on the sealing abilities of the bentonite should be assessed. Another issue arising from anaerobic corrosion of C-steel is H_2 production at a high rate. H_2 solubility in water is limited, and mass transport of dissolved species through compacted bentonite is very slow. Consequently, a gas phase may be formed that could affect the properties of bentonite.[40,43]

After container failure, the degraded C-steel becomes a constraint to radionuclide release from the waste form and subsequent migration through the EBS. The corrosion products play a significant role in this process.[47]

Localized Corrosion

Pitting and crevice corrosion of C-steel may only occur in the classic sense if the metal is passivated. Passivation of C-steel in bentonite pore water is unlikely.[39] However, considering uncertainties in the disposal environment localized corrosion cannot be fully excluded. C-steel is reported to be passive when in contact with some kind of clays.[48] Passivation in CO_3^{2-}/HCO_3^- solutions is expected at pH > 9–9.5. E_P and especially E_{RP} of C-steel in aqueous solutions containing CO_3^{2-}, HCO_3^-, and Cl^- are closed to the passivation potential. This fact suggests that localized corrosion would be possible in the aerobic stage.[49] However, the limited amount of O_2 in compacted bentonite may preclude further propagation of localized corrosion. A certain degree of localized corrosion allowance might be tolerated until the O_2 is exhausted without compromising the integrity of the container.[39]

In unbackfilled conditions, localized corrosion may occur as a consequence of a nonuniformly wetted surface during saturation. Deliquescent salts on the container surface may lead to the formation of water droplets connected by a thin adsorbed water layer. Oxygen reduction occurs on the periphery of the droplet, while anodic dissolution occurs in the center of the droplet. This degradation mechanism may be operative only during the aerobic stage.[43]

Another localized corrosion mechanism may be operative during the aerobic-anaerobic transition. It involves the reduction of Fe^{3+} from corrosion products coupled to the dissolution of Fe at the base of pores in the underlying film.[43]

The pitting factor (PF) is defined as the ratio of the maximum depth of penetration (P) to the average depth of penetration (X). For C-steels, PF decreases as the average depth of penetration increases (Fig. 5). Equation 8 allows the calculation of P (in mm) as a function of X (in mm). This equation was obtained from extreme values statistical analyses of experimental results. P = 11.9 mm is obtained by using X = 1.8 mm from the calculations for the corrosion of C-steel in the aerobic stage. This approach was developed for the assessment of the degree localization of the general attack, not for classic pitting corrosion. However, it is stated that the maximum depth of penetration obtained by Eq. 8 is conservative even if pitting and crevice corrosion occur.[39]

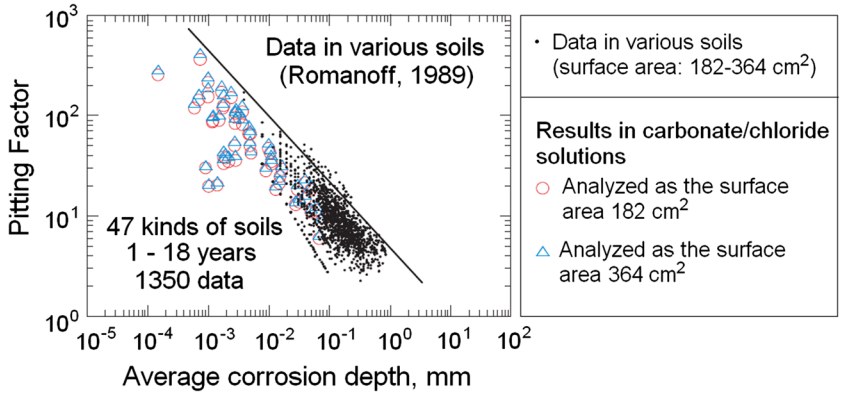

Fig. 5. Pitting factor as a function of the average corrosion depth (adapted from Ref. 39).

$$P\,[\mathrm{mm}] = X + 7.5X^{0.5} \tag{8}$$

$$2H^+ + 2e^- \rightarrow H_2 \tag{9}$$

$$2H_2O + 2e^- \rightarrow H_2 + 2OH^- \tag{10}$$

Stress-Corrosion Cracking

C-steel may suffer SCC in a variety of environments such as concentrated phosphate or nitrate solutions, or high-temperature water. However, most of these environments are not relevant for repository conditions. Cracking due to the presence of carbonate/bicarbonate solutions is the most relevant condition for the SCC of C-steel containers in clay environment. The carbonate/bicarbonate SCC appears in two forms defined by precise ranges of pH and potential. Near-neutral pH SCC occurs in dilute bicarbonate solutions with $5.5 < \mathrm{pH} < 7.5$ and potentials corresponding to E_{CORR} in anaerobic environments (-0.685 to -0.715 V_{SCE}). High-pH SCC occurs in concentrated CO_3^{2-}/HCO_3^- solutions with $\mathrm{pH} > 9.3$ in a temperature-dependent range of potentials (-0.525 to -0.675 V_{SCE} at room temperature). Both phenomena are known from studies on pipeline steels. Near-neutral pH SCC requires cyclic loading and it is related with corrosion fatigue. High-pH SCC requires cyclic loading and crack-tip strain exceeding critical value, and it is highly temperature dependant. The carbonate/bicarbonate SCC are highly unlikely because cyclic loadings are not envisaged in the repository environment.[39,41,50]

Hydrogen-Assisted Cracking

For C-steel in saturated repositories, the cathodic reaction changes from O_2 reduction to H_2 evolution Eqs. 9 and 10 at the completion of the aerobic stage. The partial pressure of H_2 at the container/bentonite interface may increase because of the slow diffusion of H_2 through the bentonite. Pressures from 6 to 10 MPa are expected. Equations 9 and 10 generate atomic hydrogen that later combines into H_2. Atomic hydrogen may absorb into the C-steel leading to cracking or blistering of the material.[39]

The critical conditions for cracking depends on a combination of applied and residual stresses, stress concentration, hydrogen uptake, and material characteristics, including the HAZ and weld metal. The critical concentration of hydrogen needed for cracking is lower as the yield strength of the material increases. The hardness of the base material and weld seams must be kept below a critical value to ensure proper resistance. The closure lid of the container may be welded without any stress relief treatment. This would lead to stresses near yield in the HAZ. Specification of low-strength C-steels (yield stress from 200 MPa to 400 MPa) avoids in a large extent the hydrogen-related degradation modes. Hydrogen-induced cracking (HIC) and stress-oriented hydrogen induced cracking (SOHIC) are considered the most likely mechanisms for low-strength C-steels. HIC may be minimized or avoided by specifying materials with low S and Mn (low inclusions). It is claimed that HIC is not expected for C-steels at $\mathrm{pH} > 6$.[12,39,51]

Because of the high diffusivity of hydrogen in ferrite, it is expected to diffuse through the container wall developing an internal H_2 atmosphere. It has been stated that HIC is more likely to initiate from the inside of the container.[51]

Microbiologically Influenced Corrosion

C-steel is susceptible to MIC under both aerobic and anaerobic conditions. Sulfate-reducing and acid-producing bacteria are commonly associated with this phenomenon. Corrosion rates up to 0.3 mm/year have been reported for C-steel under MIC in special cases.[45] Biofilm formation is not expected in compacted bentonite.[37,43] MIC is an important degradation mode to be assessed by the

Table I. Advantages of the emplacement of C-steel waste containers in bentonite backfill versus unbackfilled argillaceous environment

C-steel in bentonite backfill	C-steel in unbackfilled argillaceous environment
Shorter aerobic stage due to lower O_2 inventory within the repository	Retrievability of containers
Active general corrosion precludes localized corrosion	Unfavorable C-steel/clay interaction due to Fe^{2+} in montmorillonite and H_2 gas phase formation are minimized
MIC is avoided	Lower anaerobic corrosion rates due to higher quality film of corrosion products. Possible passivation
	Lower H_2 pressure reduces the risk of HIC

unbackfilled French repository model. However, it should be considered that the mere presence of microorganisms in the repository does not necessarily lead to biodegradation. Only those microorganisms that affect the anodic or cathodic reactions are relevant.[12,37]

Radiation Effects

Gamma radiation fields may produce oxidizing agents. The corrosion rate of C-steel has been observed to increase in some cases and to decrease in other cases under radiation fields. The threshold dose rate of 3 Gy/h has been set for C-steel in seawater to have an effect on the corrosion rate. Higher corrosion rates have been reported for C-steel irradiated at 11 Gy/h and 300 Gy/h when compared to nonirradiated material. A thick-walled container minimizes the effect of radiation.[41,43,52]

Bentonite Backfill Versus Unbackfilled Argillaceous Groundwater

The C-steel waste containers in contact with compacted bentonite (e.g., Swiss and Japanese models) and with groundwater from argillaceous rock (French model) are prone to the same degradation processes. However, the different repository designs have their advantages, which are listed in Table I.

Corrosion of C-Steel in Concrete

General Corrosion

The Belgian repository may be placed in Boom clay, and its design relies in the supercontainer concept, which includes a C-steel overpack surrounded by a thick concrete backfill. Passivation of C-steel is attained in contact with concrete due to the alkalinity of pore water. The main components of cement pore water are KOH, NaOH, and $Ca(OH)_2$. The formation of a stable Fe_3O_4 film, possibly covered by a precipitated layer of FeOOH (either lepidocrocite or goethite), is expected. The passive film is an *n*-type semiconductor due to defects in magnetite (metal interstitials and/or oxygen vacancies).[41,53]

The variables affecting the corrosion of C-steel in concrete include the relative humidity of the surrounding environment, presence of a carbonation front through the concrete which may lead to a pH decrease at the steel/concrete interface, concrete porosity, cement type, concentration ratio $[OH^-]/[Cl^-]$ at the steel/concrete interface, and the rate of diffusion of O_2 through the concrete. The main aggressive species expected in the repository is chloride. However, thiosulfate and sulfide have been considered as potentially harmful species for the anaerobic uniform corrosion of C-steel.[6,41,42,53]

E_{CORR} may be between −0.4 and −0.2 V_{SCE} in the aerobic stage and near −1.0 V_{SCE} in the anaerobic stage. Estimated corrosion rates for aerobic conditions are in the range of 0.01–0.1 μm/year. The expected corrosion rates for anaerobic conditions are even lower.[6,41,42]

Localized Corrosion

Because C-steel is passive in the concrete backfill, it may be susceptible to localized corrosion below a threshold $[OH^-]/[Cl^-]$ ratio. However, it may take thousands of years before the pore water loses its alkalinity due to the low permeability of the repository. By this time, the initially trapped O_2 may have been consumed and E_{CORR} may have fallen below E_P. The probability of localized corrosion increases at high temperatures and at low $[OH^-]/[Cl^-]$ ratios. The pit depth (p, in mm) has been modeled as a function of time (t, in years) for C-steel in contact with chloride-contaminated pore water using Eq. 11. The fitted values for the constants are k = 7.3 mm/year^n and n = 0.53. The exponent near 0.5 in Eq. 11 suggests a diffusion-controlled process, such as the diffusion of O_2 though concrete.[41] The diffusion of O_2 through fully saturated pore water in concrete is very slow. Initial saturation may be of 80%, whereas full saturation is expected after 4 years of emplacement.[53]

$$p\,[\text{mm}] = k\,t^n \qquad (11)$$

Stress-Corrosion Cracking

Caustic SCC occurs typically in steam boilers operating at a high temperature (>100°C). This form of SCC is not commonly associated with C-steel in concrete. Reinforced concrete structures are not generally exposed to elevated temperatures, and the pore-water environment may be unsuitable for SCC.[43] However, both [OH^-] in cement pore water and E_{CORR} lie in the susceptibility range. Some authors claim that there is no lower temperature limit for caustic SCC to occur, but the crack velocity decreases for lower temperatures. The highest risk of SCC is on the weld seams of the container closure lids.[41]

Hydrogen-Assisted Cracking

Hydrogen production from anaerobic corrosion of C-steel may be high enough to produce a gas phase. Hydrogen diffusion through concrete pores is slow. The highest pressure expected is of 3.4 MPa after 100 years of emplacement. However, this value is considered overconservative. The occurrence of any of the HAC mechanisms for C-steel in concrete backfill is less likely than in bentonite backfill.[42]

Microbiologically Influenced Corrosion

Biofilm formation is not expected in the alkaline pore water of concrete. MIC will be an issue only after the pH at the container surface has decreased below a critical value.[43] The current simulations of the Belgian WMNP indicates a pore water pH of 13.5 during the first 200 years, which descends to pH 12.5 after 1000 years, and then to pH 11 after 80,000 years.[53]

Radiation Effects

Studies on the effect of gamma radiation on C-steel in alkaline conditions show a negligible effect of a radiation dose rate of 25 Gy/h at 25 and 80°C, with a chloride concentration up to 100 ppm.[54]

Corrosion of C-steel in Salt Brines

In the German repository model, the waste container may be in contact with salt brines. These brines are rich in chlorides and sulfates of sodium, potassium, magnesium, and calcium. The pH ranges from 4.1 to 6.9, while the initial O_2 concentration ranges from 0.6 ppm to 4.9 ppm. Only a minimal amount of water may be in contact with the containers. Temperatures of 150–200°C are expected within the first 500–1000 years of emplacement.[6]

The selected C-steel for the German program is fine-grained TStE 355 (Fe-0.17C-0.44Si-1.49Mn). This material was tested in different brines at temperatures from 90°C to 300°C. These conditions are much more aggressive than those of the near-field environment, which is expected to be dry. The ratio of volume of electrolyte to metallic surface area was 5 cm^3/cm^2. The testing time was longer than 4 years. TStE 355 C-steel was resistant to pitting corrosion, crevice corrosion, and intergranular attack (IGA) in the tested brines. The general corrosion rate of the C-steel increases with temperature, which is consistent with an acid corrosion process. An Arrhenius relationship with activation energy of 32 kJ/mol describes the corrosion rate versus temperature behavior. The material suffers uneven general corrosion, which is attributed to inhomogeneities in the steel. The nature of the corrosion products formed depends on the brine composition. Linear corrosion kinetics were found, indicating that the corrosion products are not protective. Welding causes a decrease of the localized corrosion resistance of the C-steel. However, a heat treatment of 2 h at 600°C eliminates the local corrosion attack in the welds and HAZ. TStE 355 C-steel is resistant to stress-corrosion cracking in the tested brines up to 170°C. The welding procedures do not affect the SCC resistance of the C-steel.[6,41]

Corrosion of C-Steel in the Yucca Mountain Repository

A588 weathering steel was the alternative material for the waste containers of the Yucca Mountain repository. C-steel was a concept considered in an earlier design of the repository. This low-alloy steel was proposed for a high-temperature operational mode of the repository. This operational mode delays the time before any liquid phase is in contact with the containers. The drip shields are eliminated in this design. The hot and dry conditions are thought to minimize the likelihood of localized corrosion of the containers. In this way, localized corrosion, SCC, and MIC are precluded. Depending on the position of the containers within the repository, they may operate between 350 years and 700 years before the relative humidity (RH) increase above 50%. This 50% RH was set as the threshold value for aqueous corrosion to occur. Backfilling the repository tunnels would provide an extension period of hot and dry conditions.[38]

Oxidation becomes the primary degradation mode in the above-described repository conditions. The peak temperature at the containers surface would be 280°C. A588 steel follows parabolic oxidation kinetics in air at temperatures from 500°C to 700°C, indicating that its resistance to oxidation is controlled by diffusion through a growing protective oxide layer. Extrapolation of the short-term data available results in a penetration depth of 100 μm after 1000 years at the 300°C, while the container wall thickness was expected to be 10 cm. A further assessment of the degradation modes after the hot and dry stage was not performed. The resistance of C-steel to aqueous corrosion depends on the definition of the backfilled/unbackfilled conditions.[38,55]

STAINLESS STEELS

Currently, stainless steels are not considered as reference container materials for any WMNP and they are the alternative materials of the WMNP in Belgium, United Kingdom, France and Spain.[6,12] Stainless steels have been tested in argillaceous and cementitious environments being the latter the more promising application. There is considerable amount of information regarding atmospheric corrosion of stainless steels. Austenitic stainless steels (ASS) are prone to localized corrosion and SCC in chloride-containing solutions. This susceptibility increases with temperature. Groundwater typically contains a significant amount of chlorides and HLW are heat generating. Therefore, stainless steels have been progressively abandoned as candidate materials for HLW containers. However, stainless steels are currently used as containers for intermediate-level waste in high-pH environments (concrete or other cementitious material).[6,7,56,57] Stainless steels are used to contain vitrified waste in interim dry storage conditions as described in another article in this issue of *JOM*. Duplex stainless steels (DSS) contain approximately equal proportions of austenite and ferrite. They seem to be more promising materials among the same family because of their higher strength and lower SCC susceptibility.[58]

General Corrosion

Stainless steels develop a spontaneous Cr-rich passive film in neutral and mildly acidic solutions. This film is responsible for the low general corrosion rates in a variety of environments. General corrosion is not a failure mode for stainless steels in conventional applications. However, due to the long term of HLW disposal it must be assessed by WMNP.[6,56]

The average corrosion rates of several ASS in Boom clay are between 0.003 μm/year and 0.15 μm/year. The general corrosion rates of ASS in simulated concrete pore water and cementitious environments are of the order of 0.03–0.5 μm/year, in aerobic conditions, and 0.001–0.01 μm/year, in anaerobic conditions. Corrosion rates below 0.01 μm/year are expected in the temperature range of the repository.[6] DSS show the same general corrosion behavior. In general, corrosion rates decrease with exposure time and pH, whereas they increase with temperature, chloride concentration, and degree of aeration.[58]

Localized Corrosion

Stainless steels are susceptible to localized corrosion in the forms of pitting and crevice corrosion. This susceptibility increases with temperature and chloride concentration. The dependence of E_P with chloride concentration is given by Eq. 12. The same potential versus [Cl^-] relationship is often observed for other critical potentials such as pitting and crevice corrosion repassivation potentials (E_{RP} and E_{RCREV}, respectively). The critical potentials and temperatures associated with crevice corrosion are lower than those associated with pitting corrosion.

$$E_P = A - B \log [Cl^-] \quad (12)$$

The localized corrosion resistance increases with the pitting resistance equivalent (PRE_N), which is defined in Eq. 13 as a function of the weight percentages of Cr, Mo, W, and N.[56] 304 and 316 ASS have PRE_N values between 18 and 25, whereas the DSS have PRE_N values between 30 and 35. Super DSS have $PRE_N > 40$.[56,59]

$$PRE_N = \%Cr + 3.3\,(\%Mo + 0.5\,\%W) + 16\,\%N \quad (13)$$

E_P or E_{RP} may be used for the assessment of pitting corrosion of stainless steels. E_{RP} is the potential below which a propagating pit will cease to grow, and it is more conservative than E_P. The criteria $E_{CORR} < E_P$ or $E_{CORR} < E_{RP}$ provides the safety limit for the use of stainless steels.[59]

Groundwater is considered a benign environment from a corrosion viewpoint. ASS did not suffer localized corrosion after exposures to clay environments for periods of 2–7 years, between 16°C and 170°C.[6] The species present in groundwater may have inhibitive or detrimental effects on the localized corrosion resistance of stainless steels. Hydroxide, nitrate, sulfate, carbonate, and bicarbonate are known to be beneficial anions.[60] The presence of OH^- in pore cement water inhibits localized corrosion by both decreasing E_{CORR} and increasing E_P. Therefore, E_P–E_{CORR} increases significantly with increasing pH.[58] The [OH^-]/[Cl^-] ratio is an important parameter. Types 304, 304L, 316, and 316L ASS are reported to be free from localized corrosion at [OH^-]/[Cl^-] = 0.004–0.04, in cements. Pitting corrosion of 304 ASS is reported at [OH^-]/[Cl^-] < 0.035 and 60°C. 316 ASS is free from pitting corrosion even in much more aggressive conditions. However, crevice corrosion of ASS in alkaline environments cannot be ruled out.[6,61]

Thiosulfate is considered a detrimental anion enhancing the likelihood of localized corrosion. Thiosulfate may form by the oxidation of pyrite in the clay rock during exposure to aerobic conditions or it may come from the cement grouts based on blast furnace slag. Then, it may diffuse toward the container surface.[6,62]

MnS inclusions are efficient initiation sites for pitting corrosion of stainless steels. The size and amount of inclusions should be controlled to improve the pitting corrosion resistance of the material. The existence of chromium-depleted zones around grain boundaries may result in a material more susceptible to localized corrosion. Other metallurgical factors affecting the localized corrosion resistance include σ and chi phases and δ-ferrite.[56]

The penetration depth of pitting/crevice corrosion is often observed to decrease in time. This phenomenon is called stifling, and it may result from different processes involving the local anodic and/or the cathodic kinetics.[58]

Stress-Corrosion Cracking

Stainless steels are susceptible to chloride-induced SCC. Caustic SCC of ASS is considered unlikely in a repository environment. SCC initiation is closely related to the onset of pitting or crevice corrosion because pits act as initiation sites for stress-corrosion cracks. Therefore, the SCC susceptibility decreases with increasing pH. Threshold values for SCC initiation are approximately $[OH^-]/[Cl^-] = 0.0002$ for 316 and $[OH^-]/[Cl^-] = 0.006$ for 304 ASS.[6,58]

Figure 6 shows a corrosion map for the SCC susceptibility of ASS and DSS in aerated chloride solutions as a function of temperature. Chloride-induced SCC of ASS is not observed below a threshold temperature of 40–60°C regardless of the $[Cl^-]$. This threshold temperature exceeds 100°C for 2305 and 2205 DSS. The threshold stress for cracking of DSS is also higher than for ASS.[56]

ASS and DSS are susceptible to SCC in sulfide and thiosulfate solutions. Thiosulfate enhances the deleterious effect of chloride, enabling cracking at low chloride concentrations for ASS. The severity of cracking increased with decreasing pH and with increasing thiosulfate and chloride concentrations. DSS are expected to be more resistant to cracking than ASS in sulfide and thiosulfate solutions given their enhanced resistance to chloride-induced SCC.[6,58]

Hydrogen-Assisted Cracking

High-strength stainless steels are susceptible to HAC. DSS are more susceptible to HAC than ASS because of their higher strength. Sulfide is deleterious because it leads to the poisoning of the recombination of atomic H into H_2. However, this degradation mode is unlikely for low-strength alloys in a repository environment. Passive stainless steels corrode slowly producing a low hydrogen flux in anaerobic conditions.[56,58,63]

Intergranular Attack and Welding Effects

304 ASS is susceptible to sensitization-induced IGA. Precipitation of $M_{23}C_6$ carbides during welding and other thermal treatments causes Cr depletion near grain boundaries, which increases the susceptibility to local dissolution. Low-carbon grades (e.g., 304L, 316L, etc.) that contain less than 0.03% C or stabilized grades (e.g., 321 and 347) may be used to overcome this problem.

DSS exhibit a higher resistance to sensitization and IGA than ASS. Chromium diffuses ~100 times faster in ferrite than in austenite. Therefore, Cr-depleted zones are limited to a narrow range at austenite grain boundaries. This depletion is readily reversed by rediffusion of Cr from the austenite grain.[56]

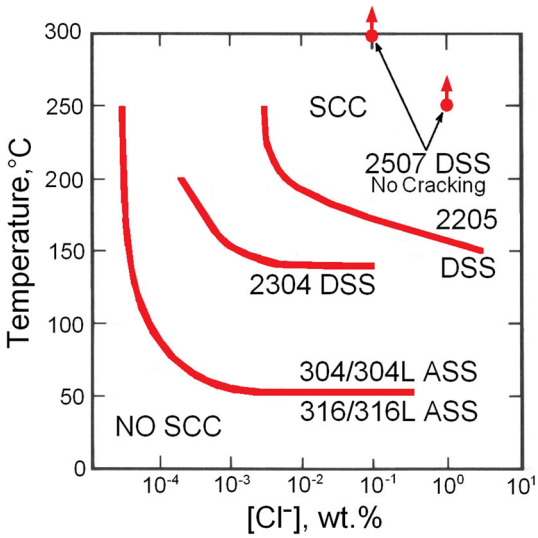

Fig. 6. SCC susceptibility of various ASS and DSS as a function of temperature and chloride concentration (adapted from Ref. 56).

Welding may affect the localized corrosion and SCC susceptibility of ASS and DSS. The selection of appropriate welding procedures and materials, and postweld heat treatment, is key to restoring the corrosion resistance of the alloy.[56]

Microbiologically Influenced Corrosion

Stainless steels are susceptible to MIC in active microbial environments. DSS are expected to be more resistant to MIC than ASS due to their higher PRE_N.[64,65] The same as for other alloys, MIC can be precluded or minimized by the appropriate selection of a backfill material (bentonite, cement, etc.).

Radiation Effects

The corrosion rates of stainless steels in a clay environment are not affected by the presence of a gamma radiation field at a dose rate of 400 Gy/h. The expected dose rates at the container surface are much lower than this value.[6,58]

Suitable Backfill

Deliquescence of salts may occur on a container's surface in unbackfilled conditions if the relative humidity falls below the deliquescence point. In these conditions, the likelihood of localized corrosion leading to atmospheric SCC is high.[57] Therefore, the use of stainless steels for HLW containers without backfill is not recommended. Bentonite backfill may provide a more benign environment. However, cementitious backfill would be the best alternative for a stainless steel container. In this environment, the most deleterious degradation modes (localized corrosion and SCC) may be avoided as long as the $[OH^-]/[Cl^-]$ ratio is kept above a threshold value.

NICKEL ALLOYS

Nickel alloys were the selected or reference container materials of the WMNP in the United States, and they are the alternative materials of the WMNP of Germany, United Kingdom, France, and Spain. The Yucca Mountain repository project considered alloy 625 (UNS N06625), alloy 825 (UNS N08825), and finally, alloy 22 (UNS N06022) for the waste container outer layer. The list of nickel alloys considered by different WMNP also includes alloys C-276 (UNS N10276) and C-4 (UNS N06455). Other alloys have been studied for comparison although not formally proposed as candidate materials: alloys C-22HS (UNS N07022), HYBRID-BC1 (UNS N10362), 59 (UNS N06059), C-2000 (UNS N06200), etc. The candidate alloys belong either to the Ni-Cr-Mo or to the Ni-Fe-Cr-Mo families. Nickel alloys may be used in saturated and unsaturated repositories, in backfill conditions, and in unbackfilled conditions. Suitable backfills include bentonite, crushed salt, and concrete. Depending on the particular repository environment, different nickel alloys may be selected considering enhanced thermal stability (alloy C-4), versatility (alloys 22, 59 and C-2000), resistance to dry oxidation (alloy 625), etc. Alloy 22 is by far the most studied nickel alloy for HLW containers.[3–11,66,67]

General Corrosion

As for stainless steels, the corrosion resistance of Ni-Cr-Mo and Ni-Fe-Cr-Mo alloys is a result of the spontaneous development of a Cr-rich passive film. This film comprises a bilayer structure consisting of a defective Cr_2O_3 that grows directly into the metal and an outer hydroxide layer. Mo and W are enriched in the outer layer and they help to maintain low currents at high passive potentials. The ionic conduction of the film is attributed to interstitial Cr^{3+} and/or O^{2-} vacancies. The passive film of alloy 22 is an *n*-type semiconductor for low passive potentials changing to *p*-type for higher potentials. This change is related to the oxidation of Cr^{3+} to Cr^{6+} within the film, and its further dissolution leads to transpassivity. The potential of the *n*-type to *p*-type transition is pH dependent. The film thickness increases with applied potential. Significant E_{CORR} ennoblement occurs when alloy 22 is immersed in aqueous solutions. The passive film properties improve with ennoblement due to higher film thickness, chromium enrichment, and film dehydration.[68–73] Figure 7 shows a summary of the passive film properties of alloy 22.[68,73]

Similarly to stainless steels, Ni-Cr-Mo and Ni-Fe-Cr-Mo alloys do not fail by general corrosion in conventional applications. The corrosion rates of alloys 22 have been measured in a variety of environments from dilute multi-ionic solutions, relevant to the Yucca Mountain repository, to acidic and very concentrated salt brines. The results range from

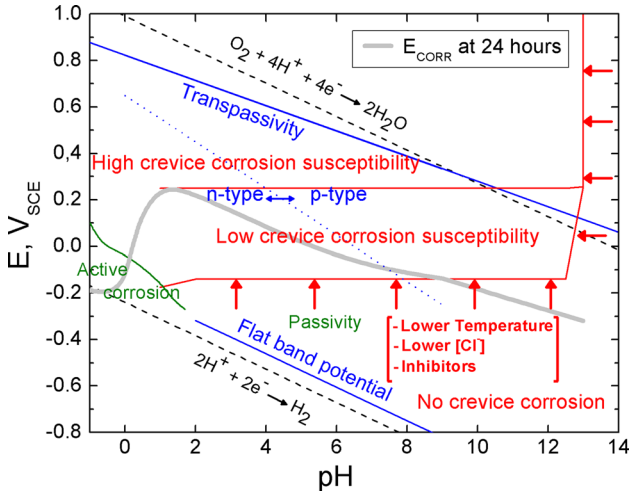

Fig. 7. Potential versus pH diagram summarizing the passive film properties and the localized corrosion susceptibility of alloy 22 in 1 mol/L NaCl at 90°C (adapted from Refs. 68,73).

0.2 μm/year after a few hours of immersion to less than 0.01 μm/year after 2–5 years of immersion, even in hot concentrated solutions.[4,70,74–76] The corrosion rate is low enough to comply with the design lifetime provided that the passive film is formed on the alloy. Depassivation of alloy 22 only occurs at low pH in hot solutions that are not envisaged in HLW repositories.[77,78] Alloy C-4 has been tested in $MgCl_2$-rich brine relevant for the German HLW repository for periods of up to 3 years. The obtained corrosion rate is 0.2 μm/year at 90°C, increasing to 0.9 μm/year at 200°C.[6]

Several processes degrading passivity have been postulated: (I) accumulation of vacancies, (II) accumulation sulfur at the alloy/film interface producing passivity breakdown followed by repassivation, which may occur several times in the lifetime of the container increasing its corrosion rate, and (III) sweeping of defects into the alloy with an adverse cumulative effect as passive dissolution progresses. These envisaged degradation processes have not been observed empirically, at least for alloy 22, but they are postulated given the long term of the application.[79]

Localized Corrosion

Most of Ni-Cr-Mo alloys do not generally suffer pitting corrosion though the less resistant Ni-Fe-Cr-Mo alloys (e.g., alloy 825) are prone to pitting corrosion in hot chloride solutions.[4,67,73,80,81] The localized corrosion resistance of nickel alloys increases with PRE_N (Eq. 13).[66,82] The absence of pitting corrosion of Ni-Cr-Mo alloys in chloride solutions is caused by the limited current density of the alloys in the acidified local solution. The maximum attainable current density is insufficient to satisfy the critical value necessary for pitting corrosion to occur.[73] Alloy 22 does not suffer pitting

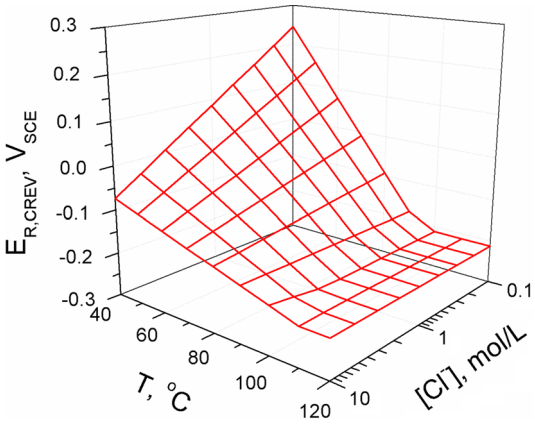

Fig. 8. Crevice corrosion repassivation potential of alloy 22 as a function of chloride concentration and temperature (adapted from Refs. 82,91).

corrosion unless very hot and concentrated chloride brines are considered.[80,83] Alloy C-4 show crevice corrosion after 3 years of exposure to $MgCl_2$-rich brine at temperatures from 90°C to 200°C and pitting corrosion only at 200°C. Localized corrosion is more severe if H_2S is added to the media.[6]

Ni-Cr-Mo alloys do not suffer localized attack in dilute multi-ionic solutions. However, they are susceptible to crevice corrosion in hot chloride solutions.[69] This susceptibility is generally measured by $E_{R,CREV}$ in the relevant environmental and metallurgical conditions. Crevice corrosion testing of alloy 22 for the Yucca Mountain repository led to significant improvement of the techniques and experimental setups used for determining E_{RCREV}. The E_{RCREV} value and its reproducibility depends on crevice former type and material used and, in a lesser extent, on the applied technique.[84–89] Like E_P, $E_{R,CREV}$ decreases for increasing $[Cl^-]$ (Eq. 12) and it decreases linearly with the temperature increase.[82,87–90] Equation 14 describes the $E_{R,CREV}$ dependence with $[Cl^-]$ and T for alloys 625, 22, C-22HS, and HYBRID-BC1, where A_1, A_2, A_3, and A_4 are constants that depend on each alloy.[91] E_{RCREV} stabilizes above a certain critical temperature reaching a minimum value, which is the E_{CORR} of the alloy in the acidified crevice solution.[82,92] Figure 8 shows E_{RCREV} for alloy 22 as a function of chloride concentration and temperature. E_{RCREV} of alloy 22 reaches its minimum above 110°C.

$$E_{RCREV} = (A_1 + A_2T)\log[Cl^-] + A_3T + A_4 \qquad (14)$$

Considering E_{RCREV} from Eq. 14 (Fig. 8) and E_{CORR} from Fig. 7, alloy 22 would be susceptible to crevice corrosion in moderately concentrated neutral chloride solutions at temperatures above 40°C. This is not observed in practical applications. The criterion of $E_{CORR} < E_{RCREV}$ for setting the safety limits regarding crevice corrosion of alloy 22 and other Ni-Cr-Mo alloys may be over conservative because of the following factors:[67,86,93–100]

- Inhibition of oxygen reduction on the passive film at the relevant potentials: Crevice corrosion of alloy 22 may initiate in open circuit conditions, but propagation is limited. Repassivation occurs because of the slow kinetics of oxygen reduction on passive alloy.[94,96,101]
- In-service crevices are significantly less demanding (severe) than those used for testing: The occurrence of crevice corrosion depends on the crevicing material and the crevice tightness. In-service "repository" crevices have not been characterized. They may not lead to crevice corrosion at all.[84,85] Regions of low and high crevice corrosion susceptibility have been defined based on the value of the crevice corrosion current density (Fig. 7). In the lower potential range, the current density is low. Therefore, only demanding crevices may lead to localized attack. In the higher potential range, the current density is maximum and constant (~20 mA/cm^2). Less demanding crevices may lead to localized attack.[73]
- Presence of inhibitors in groundwater: They reduce the environmental ranges of crevice corrosion occurrence (as indicated by the arrows of Fig. 7). Inhibitors act by increasing E_{RCREV} and by avoiding crevice corrosion above a critical [Inhibitor]/$[Cl^-]$ ratio. Nitrate is a particularly effective inhibitor found in Yucca Mountain groundwater.[60,80,97,102] However, nitrate, sulfate, and other crevice corrosion inhibitors may be consumed by microorganisms in the repository.[103] Therefore, application of the criterion of a critical [Inhibitor]/$[Cl^-]$ ratio for a complete crevice corrosion inhibition is not straightforward.
- Shallow attack: The rapid formation of polymeric molybdates in crevice corroded alloy 22 forces propagation to shift to areas unprotected by molybdate layers.[95,100]
- Crevice corrosion stifling: penetration of crevice corrosion on alloy 22 in hot chloride solutions follows Eq. 11, with $n = 0.233$. Stifling has been observed in galvanically coupled and potentiostatic conditions. The maximum penetration depth of localized attack may be limited to values significantly lower than the container thickness, as a result of stifling and repassivation of crevice corrosion.[93,98,99] It has been stated that the severity of geometrical conditions in a crevice decreases as the localized corrosion progresses.[86]

The likelihood of localized corrosion of nickel alloys is lower for saturated repositories in backfilled conditions. The conservative criterion of $E_{CORR} < E_{RCREV}$ may be applied after the initial aerobic stage.

Stress-Corrosion Cracking

Ni-Cr-Mo alloys are highly resistant to chloride-induced SCC. Alloy 22 resists SCC even in acidic concentrated and hot chloride solutions. Welded and nonwelded U-bend specimens of alloys 22, G-3, 825,

625, and C-4 exposed to pH 2.8–10 multi-ionic solutions at 60°C and 90°C have been free from cracks after 5 years of testing.[75] Alloy C-4 is immune to SCC in $MgCl_2$-rich brine at temperatures from 90°C to 200°C for periods up to 3 years. Sulfide species and lead may pose a risk to the SCC resistance of nickel alloys.[6,36,74,75,104] Alloy 22 may suffer SCC in hot bicarbonate solutions at anodic applied potentials 0.3–0.4 V higher than E_{CORR}. Chloride ions enhance bicarbonate-induced SCC. The alloy susceptibility to SCC has been related to the occurrence of an anodic peak in the polarization curves below the transpassive range.[105–107] The fulfillment of all the conditions for SCC occurrence in a repository environment is unlikely.

Thermal Stability

A long-range ordering (LRO) reaction occurs in alloy 22 above 427°C producing an ordered $Ni_2(Cr,Mo)$ phase. Topologically close-packed (TCP) phases (μ, σ, and P) precipitate between 593°C and 760°C. The LRO transformation does not affect the localized corrosion susceptibility of the alloy. However, precipitation of TCP phases, which starts at grain boundaries, may lead to alloy sensitization. TCP phases have been found in weld seams and heat-affected zones. Some authors report a detrimental effect of TCP phases on the crevice corrosion resistance of alloy 22, while others report a negligible effect. Differences are attributed to the crevice former materials used for testing. The passive behavior of alloy 22 is not affected by thermal aging.[80,87,89,108,109] Alloy C-4 shows the best thermal stability among Ni-Cr-Mo alloys.[69]

Microbiologically Influenced Corrosion

Alloy 22 has been exposed to simulated Yucca Mountain repository conditions at temperatures from 30°C to 70°C, and RH from 32% to 100%. There is no reported evidence of surface microbial activity except at the lowest temperature and highest RH, and no surface damage was observed for periods of up to 18 months. Alloy 22 is also resistant to MIC in inoculated nutrient-rich environments. MIC occurrence might enhance the general corrosion of alloy 22 without any localized effect.[37,110,111]

Radiation Effects

The exposure of alloy C-4 to $MgCl_2$-rich brine at 90°C indicates that general corrosion is not affected by gamma radiation unless very high dose rates are applied (1000 Gy/h). Localized corrosion susceptibility increases for dose rates of 10 Gy/h and above, while the resistant to SCC is not affected by gamma radiation.[6]

Alloy 22 is shielded by a 316L stainless steel inner container in the Yucca Mountain repository design. Therefore, radiation dose rates are expected to be low. The production of peroxides by radiolysis may occur though at very low concentrations.[5]

TITANIUM ALLOYS

In its last design, titanium grade 7 was the reference material for the drip shield of the Yucca Mountain repository, while titanium alloys are alternative materials of the WMNP of Germany, United Kingdom, Sweden, Japan, and Canada. Several α (hexagonal close-packed crystalline structure) and near-α titanium alloys have been proposed as corrosion-resistant barriers for HLW repositories. They include commercially pure titanium (grades 1–4), grade 5 Ti-6Al-4 V (UNS R56406), grade 6 Ti-5Al-2Sn (UNS R54250), grade 7 Ti-0.15Pd (UNS R52400), grade 12 Ti-0.3Mo-0.8Ni (UNS R53400), and grade 17 Ti-0.05Pd (UNS R52252) alloys. Titanium alloys have been selected for use in bentonite backfilled, crushed salt backfilled, and unbackfilled repositories.[6–8,39,74,112]

General Corrosion

The outstanding corrosion resistance of titanium and its alloys is caused by a TiO_2 passive film that forms spontaneously on their surface. This film is highly stable in wide ranges of potential, pH, temperature, and aqueous environments. Figure 9 shows a summary of the passive properties and localized corrosion behavior of α-titanium alloys according to Shoesmith.[8] The TiO_2 film is an n-type semiconductor whose density of donors decreases with increasing applied potentials. The dominant defects within the film are Ti^{3+} interstitials and O^{2-} vacancies. The film thickness increases with potential growing under a high-field mechanism. Crystallization of the film occurs at high temperatures (50–70°C), leading to rutile formation, and at high applied potentials (4–7 V_{SCE}), leading to anastase formation. Above 70°C, film thickening along with water absorption is observed. Water absorption improves the quality of the passive film. Hydrogen absorption occurs below a threshold potential of approximately −0.6 V_{SCE}. This is the threshold potential for the $Ti^{4+} \rightarrow Ti^{3+}$ reaction, which renders a more conductive film. Hydrogen evolution and formation of surface hydrides occur below −1 V_{SCE}. In sufficiently acidic solutions, reductive dissolution of the film occurs at cathodic potentials along with hydrogen absorption into the oxide. Palladium and other alloying elements are added to Ti alloys for enhancing cathodic proton reduction. The cathodic enhancement causes an E_{CORR} increase, thus promoting passivity. This effect is attributed to either the redeposition of dissolved Pd^{2+} or the accumulation of Pd after preferential dissolution of Ti. Proton reduction occurs at lower potentials and with smaller Tafel slopes in Pd-containing Ti alloys. Processes occurring at potentials higher than the oxygen evolution

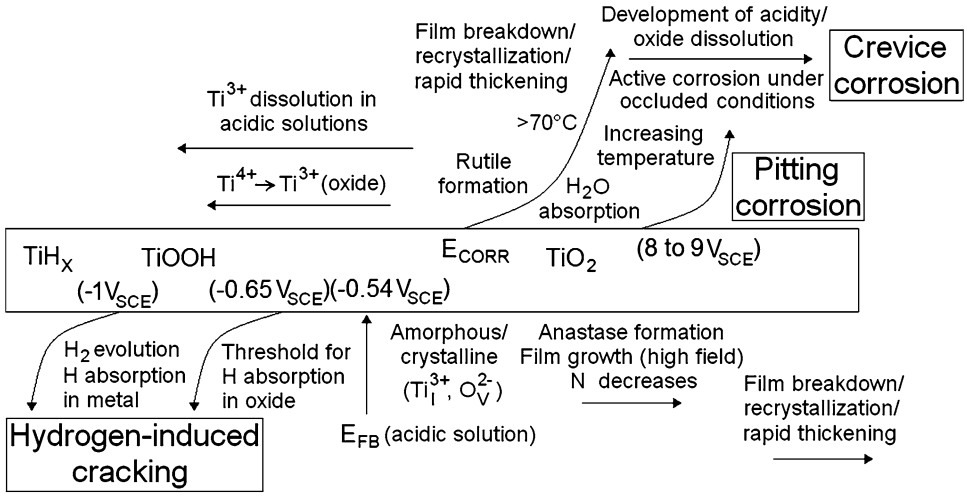

Fig. 9. Summary of the passive properties and localized corrosion behavior of α-titanium alloys (adapted from Ref. 8).

potential are not relevant for repository conditions.[7,112,113]

Corrosion rates lower than 10 nm/year are reported for Ti alloys in saline water at temperatures between 60°C and 90°C. The results in multi-ionic solutions relevant to the Yucca Mountain repository indicate an activation energy of E_A = 25.3 kJ/mol for the corrosion rate of grade 7 titanium. Studies on grade 17 titanium in concrete-permeated alkaline NaCl solutions indicate E_A = 24.6 kJ/mol. Equation 15 represents the corrosion rate of grade 17 titanium as a function of [OH^-] (mol/L) and the temperature (K), for [OH^-] < 1 mol/L.[114] According to Eq. 15, the corrosion rate of this Ti alloy increases with increasing temperature and pH. Ti-0.2Pd alloy has been tested in $MgCl_2$-rich brine relevant for the German HLW repository for periods up to 3.5 years. The results show uniform corrosion at very low rates, which declined even more with exposure time to 0.1–0.2 μm/year. No noticeable effect of temperature is reported in the range from 90°C to 200°C. Oxidation of titanium alloys in dry air observes logarithmic growth kinetics for temperatures lower than 400°C. Fluoride enhances the general corrosion of titanium alloys, and it might be present in groundwater. However, the effect of fluoride is only noticeable at high concentrations and/or in acidic conditions. General corrosion is not a main concern for these alloys in repository environments.[6,7,45,74,75,112–117]

$$\mathrm{CR}\,[\mu\mathrm{m/year}] = 3.04 \cdot 10^6 [\mathrm{OH}^-]^{0.25} \exp(-E_A/RT) \quad (15)$$

Localized Corrosion

E_{RP} for titanium alloys in 0.5 mol/L NaCl at 100°C is approximately 7 V_{SCE}, while the range of E_{CORR} values expected in a repository environment is close to 0 V_{SCE}. E_P and E_{RP} decrease with increasing temperature and chloride concentration. Pd addition and controlled Fe content lead to more resistant alloys (higher E_P and E_{RP}). Ti-0.2Pd alloy is free from any form of localized attack after testing in $MgCl_2$-rich brine at temperatures up to 200°C. Pitting corrosion is not a concern for Ti alloys in HLW repositories. However, some alloy grades are susceptible to crevice corrosion in hot chloride solutions.[6,32,39,113]

Crevice corrosion on titanium alloys tends to spread laterally. The attack progresses under the precipitated TiO_2 film that forms outside of the crevice mouth. The localized attack is supported by both the external reduction of O_2 and the internal reduction of H^+ formed by the hydrolysis of dissolved Ti^{3+}/Ti^{4+}. Hydrogen absorption occurs during crevice corrosion of titanium alloys resulting from the proton reduction within the crevice. Absorption of H under acidic conditions is easier because the oxide is thin or absent. Titanium alloys are susceptible to SCC in acidic chloride solutions such as those developed during crevice corrosion.[7,45,112,113,118,119]

The critical potential used for assessing the crevice corrosion susceptibility of titanium alloys is E_{RCREV}. The criterion of $E_{CORR} < E_{RCREV}$ is considered conservative for determining the safety limits regarding crevice corrosion.[45,120] E_{CORR} of titanium alloys during the aerobic stage in a bentonite buffered repository is given by Eq. 16, as a function of pH. E_{CORR} is insensitive to alloy composition and temperature. Therefore, E_{CORR} = 0.074 V_{SCE} is expected at pH 8, in bentonite pore water.[45] Considering the highest temperature of 90°C at the surface of the waste container, grade 1 titanium may suffer crevice corrosion above a critical NaCl concentration of [NaCl] = 0.004%, whereas grade 12 titanium may suffer crevice corrosion above [NaCl] = 0.2%. However, grades 7 and 17 alloys may not suffer crevice corrosion even in seawater at 100°C.[39,45] The less crevice corrosion resistant

titanium grades may be used as engineered barriers in saturated repositories if certain crevice corrosion propagation is allowed before oxygen is exhausted.

$$E_{CORR}(V_{SCE}) = 0.489 - 0.0591\,pH \qquad (16)$$

The corrosion penetration of grade 2 titanium in a simulated sand-buffered crystalline rock repository follows Eq. 11 with $n < 0.5$. Extrapolation of the maximum depths as a function of available O_2 indicates a maximum penetration of 2.6–2.9 mm. Although these calculations are conservative, the selection of an alloy grade more resistant to crevice corrosion is advised.[8] Creviced specimens of grade 7 titanium are reported to be free from localized attack after an 8-week exposure in multi-ionic solutions at 60°C and 105°C. Crevice corrosion of grade 7 titanium is not observed in multi-ionic solutions even at potentials of 2.5 V_{SCE} and 120°C.[6,32,39,113] Grade 17 titanium is crevice corrosion resistant in alkaline NaCl solutions. The processes included in the fabrication of containers, namely TIG welding, 20% of cold work, and a heat treatment of 4 h at 600°C, do not compromise the crevice corrosion resistance of the alloy.[114]

Stress Corrosion Cracking

Most titanium alloys exhibit excellent resistance to SCC under repository conditions regardless of applied stress, metallurgical condition, or temperature. U-bend specimens of grades 7 and 12 titanium were resistant to SCC after 4 years of exposure to multi-ionic solutions relevant to the Yucca Mountain repository. Only welded grade 12 titanium suffered cracking in one of these solutions at 90°C, whereas the nonwelded alloy was free from cracking.[75,121] U-bend specimens of Ti-0.2Pd alloy tested in $MgCl_2$-rich brine at 90°C, 170°C, and 200°C were free from SCC. It has been shown that once crack growth is initiated by low cyclic loadings, it may continue growing under constant load conditions. However, in the absence of seismic events, there is no source of dynamic loading in repositories. SCC is considered an unlikely failure mode for titanium containers in a HLW repository. It may arise only from crevice corrosion propagation after the acidic solution is developed within the crevice.[4,6,7,36,75,104,112,121]

Hydrogen-Assisted Cracking

The solubility of hydrogen in α-Ti at room temperature is in the range of 20–150 ppm, while its solubility in β-Ti is higher than 9,000 ppm. Brittle titanium hydride (TiH_2 or TiH_X) precipitates above the hydrogen solubility limit, leading to hydrogen embrittlement. Alloys with continuous β-phases provide fast diffusion paths for hydrogen and are more susceptible to HIC than alloys with a continuous α-phase. Hydrogen absorption may occur as a consequence of general corrosion under anaerobic conditions and of proton reduction in the acidic crevice environment. Threshold limits of 500–1000 ppm of absorbed hydrogen are thought to lead to HIC of α-Ti alloys.[112]

Intermetallic and Pd-containing phases within the passive film may act as windows for enhanced hydrogen absorption. For Pd-containing alloys, hydrogen absorption might occur at potentials higher than −0.6 V_{SCE}. However, the evidence for the enhancement of hydrogen absorption caused by the Pd addition is not conclusive. Relevant intermetallic compounds include Ti_2Ni and Ti_XFe, which are present in grade 12 titanium and in titanium alloys exceeding 0.03% Fe content, respectively. These compounds enhance hydrogen absorption. However, absorbed hydrogen might remain localized at the intermetallic phases unless the alloy contains β-phase ligaments that enhance the transport of hydrogen into the bulk of the alloy.[7,112]

Hydrogen absorption at temperatures of 80°C and above led to the uniform formation of hydrides on the titanium surface. These hydrides adversely affect the mechanical properties of titanium causing embrittlement. Absorption below 80°C produces layers of titanium hydride. This lath-shaped hydride forms randomly at the early stage and then forms globular hydride phases or colonies. The globular phases or colonies form eventually a layer. Cracks form on this brittle hydride layer when a critical thickness is attained. This process continues as long as the hydride layer keeps growing.[114] Nakayama et al.[45,114] performed the assessment of HIC on Ti alloys based on the thickness and mechanical properties of the hydride layer, which cracks above a critical thickness. Figure 10 shows the growth of titanium hydride phase and the formation of cracks. In anaerobic conditions, the passive current density of the titanium alloy is balanced by hydrogen evolution. Nakayama et al. calculated the fraction of the electric charge of hydrogen evolution that was associated with hydride formation. They tested a specimen under a constant applied stress of 200 MPa (simulating residual stress) in 3.5% NaCl, at 80°C, and an applied cathodic current of 0.0004 A/cm^2. At a constant cathodic current, the hydride layer thickness (d) increases in time (t) according to Eq. 17, where "a" is a constant. The hydride layer thickness of grade 17 titanium duplicates that of grade 1 titanium, which was attributed to an effect of the Pd addition. The critical hydride layer thickness for crack initiation is approximately 10–20 μm. For grade 17 titanium, the crack depth is one half of the average thickness of the hydride layer at the site of cracks. Nakayama et al. concluded that cracking is not expected after 1000 years, while a crack depth below 50 μm is expected after 10,000 years of exposure. HIC is not expected to pose a risk to the integrity of the waste containers unless large inclusions, weld cracks, or heavy cold work are present.[45,114]

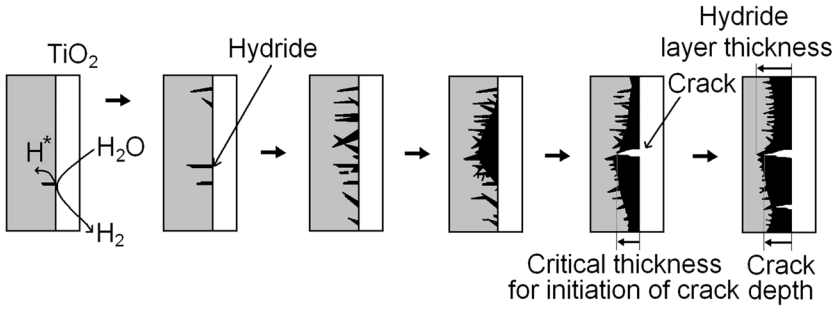

Fig. 10. Growth of titanium hydride phase and cracks (adapted from Ref. 45).

$$d = a\,t^{1/2} \tag{17}$$

Hua et al.[112] and Clarke et al.[122] performed the assessment of HIC on Ti alloys based on a threshold absorbed hydrogen content $[H]_C$ above which fast fracture occurs. Figure 11 shows schematically the combinations of stress intensity factor (K) and hydrogen concentration [H] leading to fast fracture (K_H) or slow crack growth (K_S), or to no failure. The fracture toughness of titanium alloys is not significantly reduced until $[H] > [H]_C$. $[H]_C$ increases with increasing temperature, and it decreases with increasing alloy strength. The reported values for $[H]_C$ of titanium alloys are 500–800 μg/g for grade 2 Ti, 400–600 μg/g for grade 12 Ti, and 1000–2000 μg/g for grade 16 Ti. The higher $[H]_C$ for grade 16 Ti is attributed to the prevention of hydride formation by the higher solubility of H in Pd intermetallic phases. Shoesmith et al. provided a simple model for calculating [H] in the metal as a function of time and corrosion rate. Calculations for the grade 7 titanium drip shield of Yucca Mountain repository indicate [H] = 124 μg/g after 10,000 years of emplacement, which is far less than $[H]_C$ = 1000 μg/g. These conservative calculations rule out the possibility of HIC in the anticipated repository conditions.[112]

Galvanic Corrosion

The coupling of titanium alloys to active metals, such as C-steel, could cause hydrogen absorption and eventual embrittlement of the titanium alloy. Corrosion of the coupled less-resistant material may be enhanced producing not only a higher corrosion rate but also localized corrosion. It is unlikely that galvanic corrosion potentials can be sufficiently cathodic to induce significant hydrogen absorption on titanium alloys.[112,113,123–125]

Microbiologically Influenced Corrosion

Titanium alloys are claimed to be immune to MIC. There is some speculation about H_2O_2 production within biofilms, which may lead to a significant ennoblement of Ti alloys. However, this E_{CORR} increase is not enough to initiate localized corrosion. The MIC immunity of Ti alloys is attributed to the absence of multiple oxidation states in the passive film to facilitate electron transfer during microbial metabolism. This advantage of Ti alloys over other engineered materials is significant, avoiding the need of backfill selection to minimize the effects of MIC.[37,112]

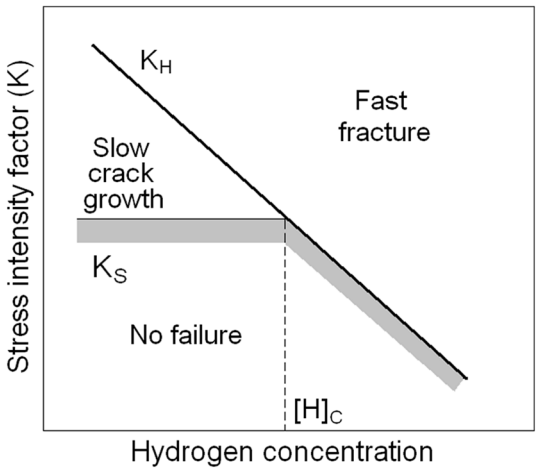

Fig. 11. Combinations of stress intensity factor and hydrogen concentration leading to fast fracture (K_H) or slow crack growth (K_S), or to no failure (adapted from Ref. 112).

Radiation Effects

Photo-induced corrosion of titanium alloys might occur under a radiation field. This phenomenon leads to oxide thinning for pH < 3 and to the accumulation of an outer layer of hydrated TiO_2 for pH > 3. Grade 12 titanium has been tested in brines under a dose rate of 150 Gy/h of gamma radiation, at temperatures from 25°C to 108°C. The results show that radiolysis products, such as H_2O_2, produce an E_{CORR} increase. In these conditions, a thicker oxide with higher anastase content is produced, while the corrosion rate is not significantly affected. These effects are attributed to H_2O_2 reduction plus other cathodic reactions and not to the gamma radiation itself on the film. Gamma radiation produces an increase of E_P of this alloy in

1 mol/L KBr at 25°C due to photoinhibition.[6,112,126,127]

The average corrosion rate of Ti-0.2Pd alloy tested in $MgCl_2$-rich brine at 90°C and under a gamma irradiation field of 1000 Gy/h is 0.7 μm/year, while in the absence of radiation, the corrosion rate is 0.17 μm/year. If the dose rate is lowered to 10 Gy/h, the corrosion rate of Ti-0.2Pd is not affected even at 150°C.[6] A gamma radiation field of 1 Gy/h does not impair the resistance of Ti grade 7 to localized corrosion and SCC in chloride brines at temperatures up to 200°C, being immune to these degradation modes. Film thickening and incorporation of groundwater cations are observed for this dose rate. No significant influence of gamma radiation has been reported for titanium alloys in a range of environments for temperatures up to 250°C.[6,112,128]

SUMMARY

Metallic engineered barriers are designed to provide a period of absolute containment to HLW in geological repositories. Candidate materials include copper alloys, carbon steels, stainless steels, nickel alloys, and titanium alloys. The national programs of nuclear waste management should identify and assess the anticipated degradation modes of the selected materials in a time-evolving environment. These degradation modes depend not only on the selected material but also on the near-field environment. The evolution of the near-field environment varies for saturated and unsaturated repositories considering backfilled and unbackfilled conditions.

Saturated repositories, located below the water table, provide an initially aerobic stage followed by a much larger anaerobic stage. The first stage is considered more aggressive because oxygen may shift the potential to high values, increasing the likelihood of localized corrosion and stress-corrosion cracking. The extent of localized corrosion, if it starts, may be limited by oxygen consumption. Titanium and nickel alloys show high critical potentials for localized corrosion, and they are resistant to stress-corrosion cracking in repository environments. Duplex and highly alloyed stainless steels may provide a similar performance at lower costs. Carbon steel and copper show a tendency to suffer general corrosion with some roughening in oxidizing conditions. In the anaerobic stage, localized corrosion is not expected, and the occurrence of stress-corrosion cracking is limited to particular materials in the presence of some aggressive species. Carbon steel, stainless steels, nickel alloys, and titanium alloys may suffer general corrosion at a very low rate. Copper is claimed to be thermodynamically immune to corrosion unless sulfides are present. Hydrogen-assisted cracking may affect carbon and stainless steels, although it may be controlled by proper alloy selection and container manufacturing. Brittle hydrides may form on titanium alloys leading to periodic cracking if the hydride layer forms.

The selection of an appropriate buffer/backfill material may help to rule out or minimize some degradation modes. Highly compacted bentonite provides a diffusion barrier to aggressive species, such as sulfide, and to reaction products, such as hydrogen. The corrosion of copper in sulfide solutions is diffusion controlled. Therefore, it occurs at a negligible rate in bentonite backfill. The water chemistry, especially pH, is controlled in bentonite pores, hindering the passivation of carbon steels, which avoids localized corrosion. Some components of bentonite react with oxygen, helping to reach the milder anaerobic conditions. However, this reaction along with the hydrogen phase formation may affect the good properties of the bentonite. Concrete or cementitious backfill provide an alkaline environment to carbon and stainless steels, ensuring passivity. Very slow general corrosion occurs as long as the high pH is maintained. Localized corrosion is avoided by the high $[OH^-]/[Cl^-]$ ratio in the aerobic stage, and it is not expected in the anaerobic stage because of the low potential. Concrete backfill may provide an unsuitable media for stress-corrosion cracking of carbon steel. Microbial activity is suppressed both in bentonite and concrete pore water. Crushed salt may be used as a backfill in a salt rock repository. The properties of this backfill are similar to those of the host rock, providing a limited amount of aqueous solution in contact with the container. The extremely high chloride content may cause localized corrosion of passive alloys in the aerobic stage. Unbackfilled saturated repositories provide a high retrievability of the waste though a higher uncertainty regarding the environment in contact with the containers. The absence of backfill reduces the unfavorable interaction of carbon steel with bentonite and the likelihood of hydrogen-assisted cracking. The presence of microbes may especially enhance general and localized corrosion in the absence of a backfill.

Unsaturated repositories, located above the water table, provide an oxidizing environment during the entire repository lifetime. Hydrogen-assisted cracking is not expected in these conditions. Localized corrosion in the form of crevice corrosion is the main anticipated degradation mode for nickel and titanium alloys. Stress-corrosion cracking is limited to very specific environmental conditions that are unlikely. The use of passive alloys ensures low corrosion rates within the entire lifetime.

Microbiologically influenced corrosion is not generally considered as a separated degradation mode but as enhancing the general and localized corrosion. An enhancement factor may be used. Radiation effects on the degradation of the metallic engineered barriers are only important for high dose rates. Radiation effects are negligible provided that a thick-walled container or an inner shielding container is used.

Carbon steel and copper alloys are the most commonly selected materials as corrosion-resistant barriers for repositories because they tend to suffer general corrosion rather than any kind of localized attack. However, passive alloys such as stainless steels, nickel alloy, and titanium alloys may provide equal performance if the engineered barrier system is properly designed.

ACKNOWLEDGEMENTS

Dr. R.M. Carranza is acknowledged for his useful comments and corrections to the original manuscript.

REFERENCES

1. International Atomic Energy Agency, *General Safety Guide No. GSG-1, Classification of Radioactive Waste* (Vienna, Austria: IAEA, 2009).
2. International Atomic Energy Agency, *Technical Report Series No. 413, Scientific and Technical Basis for the Geological Disposal of Radioactive Wastes* (Vienna, Austria: IAEA, 2003).
3. P.A. Witherspoon and G.S. Bodvarsson, eds., *Geological Challenges in Radioactive Waste Isolation: Third Worldwide Review* (Berkeley, CA: Lawrence Berkeley National Laboratory, 2001).
4. G.M. Gordon, *Corrosion* 58, 811 (2002).
5. DOE/RW-0539, *Yucca Mountain Science and Engineering Report*, 2001.
6. B. Kursten, E. Smailos, I. Azkarate, L. Werme, N.R. Smart, and G. Santarini, *State-of-the-Art Document on the Corrosion Behaviour of Container Materials—Final Report* (Brussels: European Commission, 2004).
7. F. King, *Corrosion* 69, 986 (2013).
8. D.W. Shoesmith, *Corrosion* 62, 703 (2006).
9. F. King and C. Padovani, *Corros. Eng. Sci. Technol.* 46, 82 (2011).
10. J.-M. Gras, *C. R. Phys.* 3, 891 (2001).
11. D. Féron, D. Crusset, and J.-M. Gras, *J. Nucl. Mater.* 379, 16 (2008).
12. D. Féron, D. Crusset, and J.-M. Gras, *Corrosion* 65, 213 (2009).
13. N. Sridhar and G.A. Cragnolino, *Corrosion* 49, 967 (1993).
14. R.O. Cassibba and S.A. Fernández, *J. Nucl. Mater.* 161, 93 (1989).
15. ASTM G 82-98, Standard in *Annual Book of ASTM Standards Vol. 03.02, Corrosion of Metals; Wear Erosion* (Philadelphia, PA: ASTM International, 2013).
16. A.B. Svensk Kärnbränslehantering, *TR-90, Copper as Canister Material for Unreprocessed Nuclear Waste—Evaluation with Respect to Corrosion* (Stockholm, Sweden: Svensk Kärnbränslehantering AB, 1978).
17. F. King, L. Ahonen, C. Taxén, U. Vuorinen, and L. Werme, *TR-01-23 Copper Corrosion Under Expected Conditions in a Deep Geologic Repository* (Stockholm, Sweden: Svensk Kärnbränslehantering AB, 2001).
18. F. King, M. Kolar, and P. Maak, *J. Nucl. Mater.* 379, 133 (2008).
19. F. King, C. Lilja, and M. Vähänen, *J. Nucl. Mater.* 438, 228 (2013).
20. F. King, M. Kolar, M. Vähänen, and C. Lilja, *Corros. Eng. Sci. Technol.* 46, 217 (2011).
21. B. Rosborg and J. Pan, *Electrochim. Acta* 53, 7556 (2008).
22. J. Chen, Z. Qin, and D.W. Shoesmith, *Corros. Eng. Sci. Technol.* 46, 138 (2011).
23. J. Chen, Z. Qin, and D.W. Shoesmith, *Electrochim. Acta* 56, 7854 (2011).
24. J.M. Smith, Z. Qin, F. King, and D.W. Shoesmith, *Sulphur-Assisted Corrosion in Nuclear Disposal Systems*, ed. D. Féron, K. Bruno, and F. Druyts (Leeds, U.K.: European Federation of Corrosion by Maney Publishing, 2011), pp. 109–123.
25. J. Smith, Z. Qin, F. King, L. Werme, and D.W. Shoesmith, *Corrosion* 63, 135 (2007).
26. G. Hultquist, *Corros. Sci.* 26, 173 (1986).
27. G. Hultquist, G.K. Chuah, and K.L. Tan, *Corros. Sci.* 29, 1371 (1989).
28. G. Hultquist, M.J. Graham, P. Szakalos, G.I. Sproule, A. Rosengren, and L. Gråsjö, *Corros. Sci.* 53, 310 (2011).
29. P. Szakálos, G. Hultquist, and G. Wikmark, *Electrochem. Solid State Lett.* 10, C63 (2007).
30. M. Bojinov, I. Betova, and C. Lilja, *Corros. Sci.* 52, 2917 (2010).
31. F. King and C. Lilja, *Corros. Eng. Sci. Technol.* 46, 153 (2011).
32. Z. Szklarska-Smialowska, *Pitting and Crevice Corrosion* (Houston, TX: NACE International, 2005), pp. 327–346.
33. N. Taniguchi and M. Kawasaki, *J. Nucl. Mater.* 379, 154 (2008).
34. E. Arilahti, T. Lehtikuusi, M. Olin, T. Saario, and P. Varis, *Corros. Eng. Sci. Technol.* 46, 134 (2011).
35. F. King and R.C. Newman, *TR-10-04 Stress Corrosion Cracking of Copper Canisters* (Stockholm, Sweden: Svensk Kärnbränslehantering AB, 2010).
36. R.B. Rebak, *Corrosion/2013* (Houston, TX: NACE International, 2013), Paper No. 2597.
37. F. King, *Corrosion* 65, 233 (2009).
38. J.S. Armijo, P. Kar, and M. Misra, *Nucl. Eng. Des.* 236, 2589 (2006).
39. Japan Nuclear Cycle, *JNC, H12: Project to Establish the Scientific and Technical Basis for HLW Disposal in Japan, Supporting Report 2, Repository Design and Engineering Technology* (Tokai, Japan: Japan Nuclear Cycle, 2000).
40. D. Landolt, A. Davenport, J.H. Payer, and D.W. Shoesmith, *Technical Report 09-02, A Review of Materials and Corrosion Issues Regarding Canisters for Disposal of Spent Fuel and High-Level Waste in Opalinus Clay* (Wettingen, Switzerland: NAGRA, 2009).
41. N.R. Smart, *Corrosion* 65, 195 (2009).
42. S. Wickham, *Report NIROND-TR 2007-07E, Evolution of the Near-Field of the ONDRAF/NIRAS Repository Concept for Category C Wastes* (Fleurus, Belgium: ONDRAF/NIRAS, 2008).
43. F. King, *Report NWMO TR-20007-01, Overview of a Carbon Steel Container Corrosion Model for a Deep Geological Repository in Sedimentary Rock* (Toronto, Ontario, Canada: Nuclear Waste Management Organization, 2007).
44. N. Taniguchi, *Predicting Long Term Corrosion Behavior in Nuclear Waste Systems*, ed. D. Féron and D.D. Macdonald (London, U.K.: European Federation of Corrosion by Maney Publishing, 2003), pp. 424–438.
45. G. Nakayama, N. Nakamura, Y. Fukaya, M. Akashi, and H. Ueda, *Predicting Long Term Corrosion Behavior in Nuclear Waste Systems*, ed. D. Féron and D.D. Macdonald (London, U.K.: European Federation of Corrosion by Maney Publishing, 2003), pp. 373–394.
46. L. Johnson and F. King, *J. Nucl. Mater.* 379, 9 (2008).
47. I.G. McKinley, F.B. Neall, E.M. Scourse, and H. Kawamura, *Scientific Basis for Nuclear Waste Management XXXV, Vol. 1475*, ed. G.S. Duffó, R.M. Carranza, and R.B. Rebak (New York: Cambridge University Press, 2012), pp. 281–286.
48. F.A. Martin, C. Bataillon, and M.L. Schlegel, *J. Nucl. Mater.* 379, 80 (2008).
49. C.S. Brossia and G.A. Cragnolino, *Corrosion* 56, 505 (2000).
50. F. King, *Report TR-2010-21, Stress Corrosion Cracking of Carbon Steel Used Fuel Containers in a Canadian Deep Geological Repository in Sedimentary Rock* (Toronto, ON, Canada: Nuclear Waste Management Organization, 2010).
51. A. Turnbull, *Technical Report 09-04, A Review of Possible Effects of Hydrogen on Lifetime of Carbon Steel Nuclear Waste Canisters* (Wettingen, Switzerland: NAGRA, 2009).

52. N.R. Smart, A.P. Rance, and L.O. Werme, *J. Nucl. Mater.* 379, 97 (2008).
53. B. Kursten, F. Druyts, D.D. Macdonald, N.R. Smart, R. Gens, L. Wang, E. Weetjens, and J. Govaerts, *Corros. Eng. Sci. Technol.* 46, 91 (2011).
54. B.J. Winsley, N.R. Smart, A.P. Rance, P.A.H. Fennel, B. Reddy, and B. Kursten, *Corros. Eng. Sci. Technol.* 46, 111 (2011).
55. Y.-N. Chang, *Corrosion* 50, 3 (1994).
56. A.J. Sedriks, *Corrosion of Stainless Steels* (New York, NY: Wiley, 1996).
57. J.-I. Tani, M. Mayuzumi, and N. Hara, *Corrosion* 65, 187 (2009).
58. F. King, *Corrosion Resistance of Austenitic and Duplex Stainless Steels in Environments Related to UK Geological Disposal, A Report to NDA RWMD* (Cumbria, U.K.: Nuclear Decommissioning Authority, Radioactive Waste Management Directorate, 2009).
59. Z. Szklarska-Smialowska, *Pitting and Crevice Corrosion* (Houston, TX: NACE International, 2005).
60. M.A. Rodríguez, *Corros. Rev.* 30, 19 (2012).
61. S. Wang and R.C. Newman, *Corrosion* 60, 448 (2004).
62. B. Kursten and F. Druyts, *Corrosion/2000* (Houston, TX: NACE International, 2000), Paper 00201.
63. D. Féron, *Sulphur-Assisted Corrosion in Nuclear Disposal Systems*, ed. B. Kursten, F. Druyts, and D. Féron (Wakefield, U.K.: Maney Publishing, 2011), pp. 66–80.
64. F. Mansfeld and B. Little, *Corros. Sci.* 32, 247 (1991).
65. P.J. Antony, S. Chongdar, P. Kumar, and R. Raman, *Electrochim. Acta* 52, 3985 (2007).
66. N.S. Zadorozne, C.M. Giordano, M.A. Rodríguez, R.M. Carranza, and R.B. Rebak, *Electrochim. Acta* 76, 94 (2012).
67. R.M. Carranza, *JOM* 60, 58 (2008).
68. M.A. Rodríguez and R.M. Carranza, *J. Electrochem. Soc.* 158, C221 (2011).
69. R.B. Rebak, *Materials Science and Engineering: A Comprehensive Treatment*, ed. R.W. Cahn, P. Haasen, and E.J. Kramer (Weinheim, Germany: Wiley-VCH, 2000).
70. A.C. Lloyd, D.W. Shoesmith, N.S. McIntyre, and J.J. Noël, *J. Electrochem. Soc.* 150, B120 (2003).
71. A.C. Lloyd, J.J. Noël, S. McIntyre, and D.W. Shoesmith, *Electrochim. Acta* 49, 3015 (2004).
72. D.D. Macdonald, *J. Nucl. Mater.* 379, 24 (2008).
73. M.A. Rodríguez, R.M. Carranza, and R.B. Rebak, *Corrosion* 66, 015007 (2010).
74. F. Hua and G.M. Gordon, *Corrosion* 60, 764 (2004).
75. R.B. Rebak, *Corrosion* 65, 252 (2009).
76. M.A. Rodríguez, R.M. Carranza, and R.B. Rebak, *Metall. Mater. Trans. A* 36, 1179 (2005).
77. M.A. Rodríguez, R.M. Carranza, and R.B. Rebak, *J. Electrochem. Soc.* 157, C1 (2010).
78. J.J. Gray and C.A. Orme, *Electrochim. Acta* 52, 2370 (2007).
79. A.A. Sagüés and C.A.W. Di Bella, eds., *Proceedings from an International Workshop on Long-Term Passive Behavior, July 19–20, 2001, Arlington, Virginia* (Arlington, VA: U.S. Nuclear Waste Technical Review Board, 2001).
80. R.B. Rebak, *Corrosion/2005* (Houston, TX: NACE International, 2005), Paper 05610.
81. G.A. Cragnolino and N. Sridhar, *Corrosion* 47, 464 (1991).
82. E.C. Hornus, C.M. Giordano, M.A. Rodríguez, and R.M. Carranza, *MRS Symp. Proc. Vol. 1475, Scientific Basis in Nuclear Waste Management XXXV*, ed. R.M. Carranza, G.S. Duffó, and R.B. Rebak (New York, NY: Cambridge University Press, 2012), pp. 477–482.
83. M.A. Rodríguez, M.L. Stuart, and R.B. Rebak, *Corrosion/2007* (Houston, TX: NACE International, 2007), Paper 07577.
84. C.M. Giordano, M. Rincón Ortíz, M.A. Rodríguez, R.M. Carranza, and R.B. Rebak, *Corros. Eng. Sci. Technol.* 46, 129 (2011).
85. X. Shan and J.H. Payer, *Corrosion* 66, 105005 (2010).
86. M. Rincón Ortíz, M.A. Rodríguez, R.M. Carranza, and R.B. Rebak, *Corrosion* 66, 105002 (2010).
87. K.J. Evans, A. Yilmaz, S.D. Day, L.L. Wong, J.C. Estill, and R.B. Rebak, *JOM* 57, 56 (2005).
88. A.K. Mishra and G.S. Frankel, *Corrosion* 64, 836 (2008).
89. D. Dunn, Y. Pan, K.-T. Chiang, L. Yang, G.A. Cragnolino, and X. He, *JOM* 57, 49 (2005).
90. R.M. Carranza, M.A. Rodríguez, and R.B. Rebak, *Corrosion* 63, 480 (2007).
91. E.C. Hornus, C.M. Giordano, M.A. Rodríguez, R.M. Carranza, and R.B. Rebak, *Corros. Sci.*, in press.
92. S. Sosa Haudet, M.A. Rodríguez, and R.M. Carranza, *MRS Symp. Proc. Vol. 1475, Scientific Basis for Nuclear Waste Management XXXV*, ed. R.M. Carranza, G.S. Duffó, and R.B. Rebak (New York, NY: Cambridge University Press, 2012), pp. 489–494.
93. A. Yilmaz, P. Pasupathi, and R.B. Rebak, *ASME Press. Vessel. Pip. Conf.* (New York, NY: ASME, 2005), Paper PVP2005-71174.
94. P. Jakupi, J.J. Noel, and D.W. Shoesmith, *Corros. Sci.* 53, 3122 (2011).
95. P. Jakupi, J.J. Noël, and D.W. Shoesmith, *Corros. Sci.* 54, 260 (2012).
96. M.A. Rodríguez, R.M. Carranza, and R.B. Rebak, *Corrosion/2009* (Houston, TX: NACE International, 2009), Paper 09424.
97. M. Rincón Ortíz, M.A. Rodríguez, R.M. Carranza, and R.B. Rebak, *Corros. Sci.* 68, 72 (2013).
98. X. He and D.S. Dunn, *Corrosion* 63, 145 (2007).
99. X. He, D.S. Dunn, and A.A. Csontos, *Electrochim. Acta* 52, 7556 (2007).
100. P. Jakupi, F. Wang, J.J. Noël, and D.W. Shoesmith, *Corros. Sci.* 53, 1670 (2011).
101. M.L. Ungaro, M.A. Rodríguez, R.M. Carranza, and R.B. Rebak, *Corrosion/2014* (Houston, TX: NACE International, 2014), Paper C2014-3904.
102. B.A. Kehler, G.O. Ilevbare, and J.R. Scully, *Corrosion* 57, 1042 (2001).
103. B.J. Little, *Corrosion* 59, 701 (2003).
104. P.L. Andresen, P.W. Emigh, L.M. Young, and G.M. Gordon, *Corrosion/2001* (Houston, TX: NACE International, 2001), Paper 01130.
105. P.K. Shukla, D.S. Dunn, K.-T. Chiang, and O. Pensado, *Corrosion/2006* (Houston, TX: NACE International, 2006), Paper 06502.
106. K.T. Chiang, D.S. Dunn, and G.A. Cragnolino, *Corrosion* 63, 940 (2007).
107. N.S. Zadorozne, R.M. Carranza, C.M. Giordano, A.E. Ares, and R.B. Rebak, *Corrosion/2012* (Houston, TX: NACE International, 2012), Paper C2012-0001413.
108. D.S. Dunn, Y.-M. Pan, L. Yang, and G.A. Cragnolino, *Corrosion* 62, 3 (2006).
109. R.M. Carranza, M.A. Rodríguez, and R.B. Rebak, *Corrosion/2008* (Houston, TX: NACE International, 2008), Paper 08579.
110. J.M. Horn, S. Martin, B. Maaterson, and T. Lian, *Corrosion/99* (Houston, TX: NACE International, 1999), Paper 162.
111. J. Horn, T. Lian, and S. Martin, *Corrosion/2002* (Houston, TX: NACE International, 2002), Paper 02448.
112. F. Hua, K. Mon, P. Pasupathi, G. Gordon, and D. Shoesmith, *Corrosion* 61, 987 (2005).
113. R.W. Schutz and D.E. Thomas, *ASM Handbook* (Materials Park, OH: ASM International, 1996), pp. 669–706.
114. G. Nakayama, Y. Sakakibara, and S. Kawakami, *Corros. Eng. Sci. Technol.* 46, 159 (2011).
115. G.T. Burstein and A.J. Davenport, *J. Electrochem. Soc.* 136, 936 (1989).
116. N. Sato, *Corros. Sci.* 31, 1 (1990).
117. C.S. Brossia and G.A. Cragnolino, *Corrosion* 57, 768 (2001).
118. X. He, J.J. Noël, and D.W. Shoesmith, *Corros. Sci.* 47, 1177 (2005).
119. L. Yan, J.J. Noël, and D.W. Shoesmith, *Electrochim. Acta* 56, 1810 (2011).

120. M. Akashi, G. Nakayama, and T. Fukuda, *Corrosion/98* (Houston, TX: NACE International, 1998), Paper 158.
121. D.V Fix, J.C. Estill, L.L. Wong, and R.B. Rebak, *Corrosion/2004* (Houston, TX: NACE International, 2004), Paper 04551.
122. C.F. Clarke, D. Hardie, and B.M. Ikeda, *Corros. Sci.* 39, 1545 (1997).
123. K. Azumi and M. Seo, *Corros. Sci.* 45, 413 (2003).
124. A.K. Roy and D.L. Fleming, *Corrosion/98* (Houston, TX: NACE International, 1998), Paper 156.
125. A.K. Roy and D.L. Fleming, *Corrosion/99* (Houston, TX: NACE International, 1999), Paper 465.
126. Y.J. Kim and R.A. Oriani, *Corrosion* 43, 85 (1987).
127. Y.J. Kim and R.A. Oriani, *Corrosion* 43, 92 (1987).
128. A. Michaelis, S. Kudelka, and J.W. Schultze, *Electrochim. Acta* 43, 119 (1998).